The Making of DFS 5.1

R. Dussin, B. Barnier *

February 18, 2013

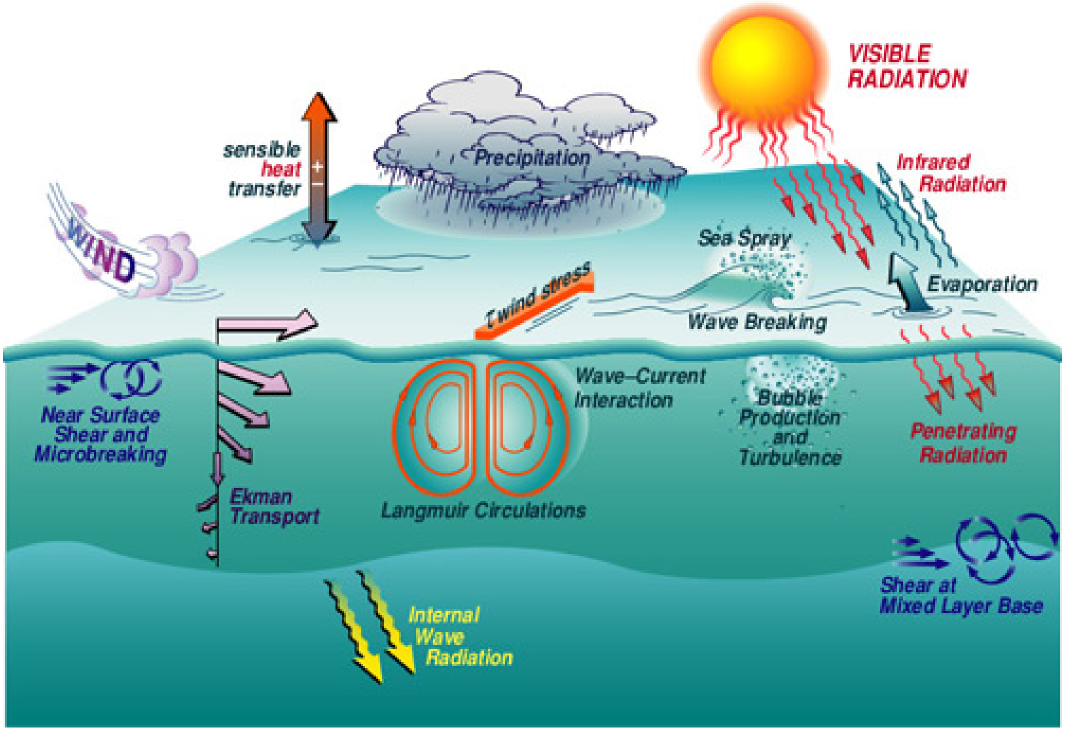

*LEGI, CNRS-UJF-INPG-OSUG, Grenoble, France

Contents

1 Prologue : on the utility to correct ERA-interim

ERA-interim is the latest reanalysis provided by ECMWF. It covers the period 1979-2010 and will be updated for following years. A lot of improvements have been implemented to both the atmospheric model and data assimilation system compared to ERA-40, which was the basis for DRAKKAR Forcing Set 4.3 (hereafter DFS4.3). The spatial and temporal resolution have also been improved (0.7° and 3-hourly for ERA-interim, 1.125° and 6-hourly for ERA-40). Despite a better representation of the atmospheric state, the reanalysis still has some flaws when forcing an ocean general circulation model, which has been identified with the global 1/4° global configuration ORCA025, based on NEMO code.

Gyre intensity Figure 1 shows the transport across the Florida-Bahamas section, which is a good proxy for North-Atlantic subtropical gyre intensity. This section is monitored and observations (in blue) are available since 1982. We compare a DFS4.3 forced ORCA025 simulation (in black) and an ERA-interim forced ORCA025.L75 simulation (in red). The transport collapses in the ERA-interim forced simulation, which is the result of a weakening of the subtropical gyre circulation. This behavior is observed in a large number of ERA-interim forced simulation performed by the DRAKKAR group and is not due to vertical resolution nor spin-up. Hence we can conclude that gyre circulation has to be strengthen, which can be achieved by increasing the wind module.

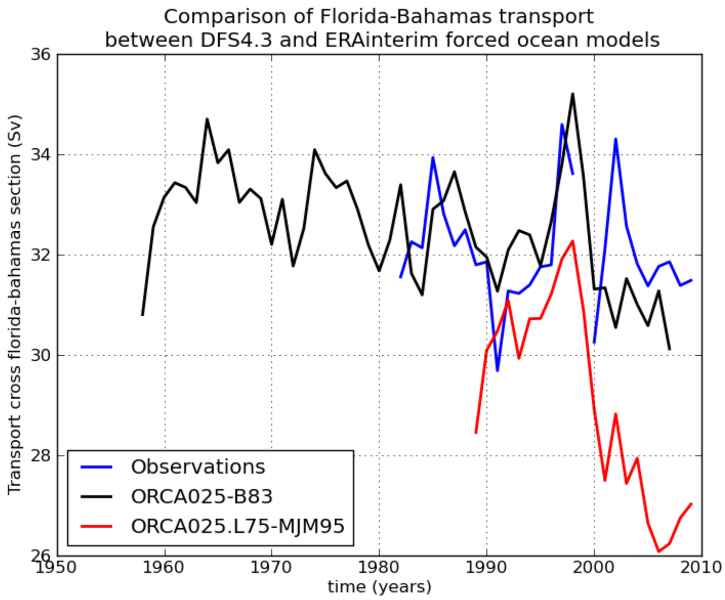

Figure 1: Comparison of the Florida-Bahamas transport for DFS4.3 and ERAinterim forced model

Freshwater input Figure 2 shows the sea surface salinity restoring term in an ERA-interim ORCA025.L75 forced simulation. We can identify several area where the restoring term is important : the western equatorial pacific and indian ocean, the equatorial atlantic and along US/Canada east coast. The precipitations are intense and likely to be overestimated at low latitudes and underestimated at mid-latitudes (we found similar results when comparing ERA-interim to DFS4.3 satellite-based precipitations). ERA-interim provides daily precipitations at 0.7° resolution, which brings more variability to the system than the monthly satellite-based precipitations of DFS4.3. However, to be useful, the precipitations need to be in good agreement with observations. Hence a major issue is to decrease precipitations at low-latitude which will affect global hydrological cycle, which is already unbalanced in ERAinterim (E-P-R = 0.33 mm/day). Despite of this non-balanced freshwater budget, free (without sea surface salinity restoring) simulations forced by ERA-interim have an important negative salinity drift, leading to sea surface rise of 50-60cm in 20 years in both ORCA246 and ORCA025.

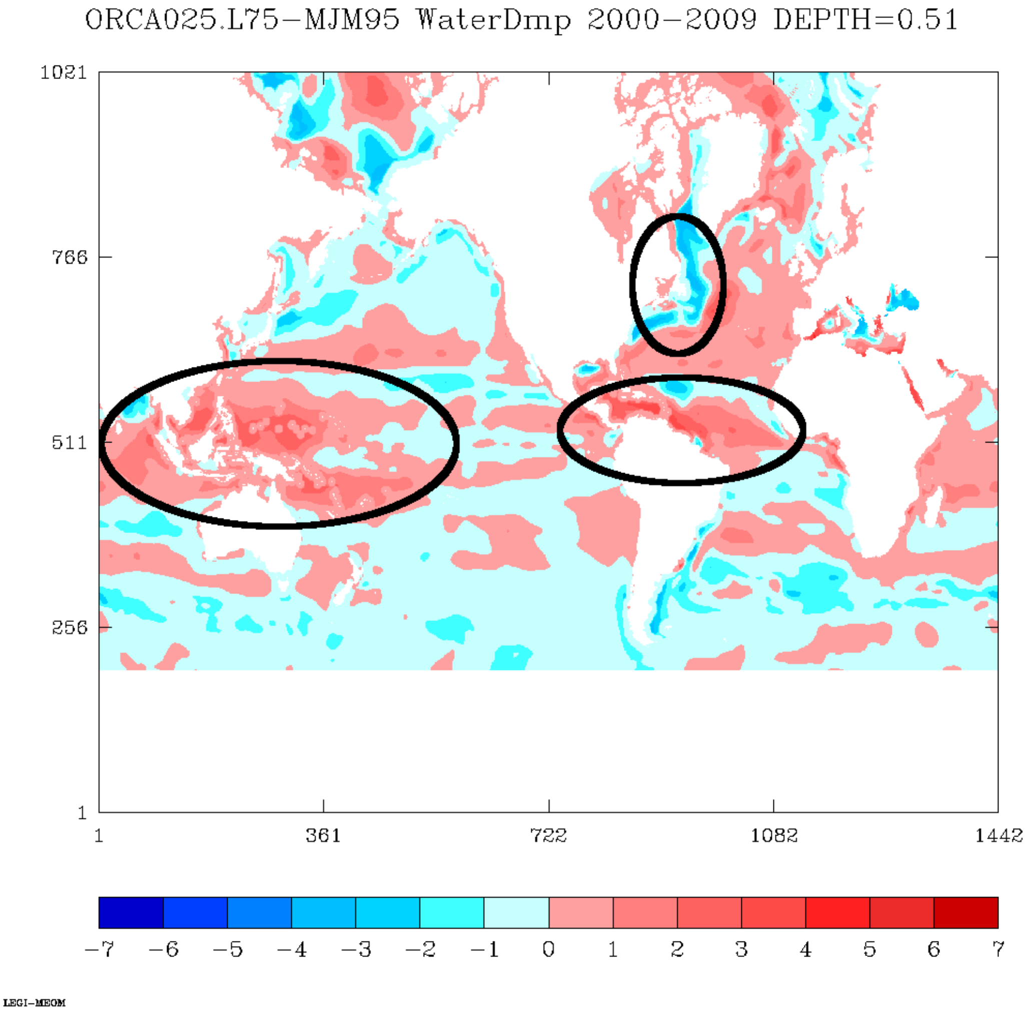

Figure 2: Mean Sea Surface Salinity restoring term in an ERA-interim forced simulation (2000-2009) Positive (red) values means that the restoring acts similarly as evaporation, negative (blue) values means the restoring bring freshwater.

Radiative fluxes ERA-interim also provides daily radiative fluxes at 0.7° resolution, whereas satellite-based DFS4.3 radiative fluxes have only 2.5° resolution. However ERA-interim shortwave radiation are likely to be overestimated, in particular in eastern part of ocean basins if we compare them to DFS4.3 (cf figure 3). In those regions, we see that the longwave radiation has opposite sign compared to shortwave which can be due to bad cloud cover representation. The signature of such discrepancies is difficult to characterize with sensitivity simulation as wind forcing also acts a lot on heat budget.

In this report, we will explain in a first section how the modifications were performed on ERA-interim. We will first explain briefly how we have corrected t2/q2 in the arctic and the benefits on sea-ice obtained in a coarse-resolution model. This modifications is very local and does not affect much the global balances. Secondly, we will discuss more precisely the method chosen for the wind reinforcement, which will bring lot of changes on heat and freshwater budget. Then the third part is related to corrections on radiative fluxes. The results of those corrections on global heat balance are of -7 W/m2 (from +5 to -2 W/m2) which is important if we compare to global warming (which estimates are +0.5 W/m2 perturbation on the system) but it is in the error bar of air-sea fluxes. Finally, we conclude with the corrections on precipitations which was a difficult task as spatial corrections were needed as well as trying to close the freshwater budget. In the second section, we will provide to the reader a full atlas of differences between DFS5.1 and ERAinterim for each atmospheric variable, focusing on the climatological mean (map of differences, zonal means and its difference) as the well the interannual timeserie. The reader which needs more detailed information can ask the authors for the so-called FARC (Flux Atlas Revolutionary Computation) report which provides several maps, timeseries and trends for each flux and atmospheric variable. Then we will conclude the story with a summary, additional information on fluxes and some remarks.

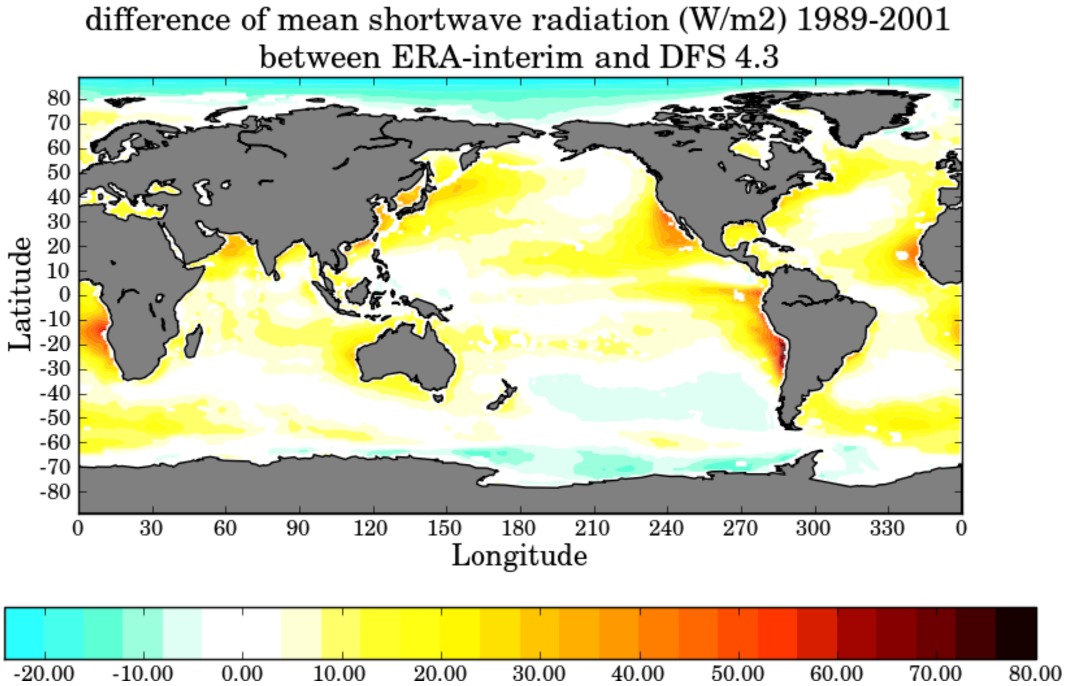

Figure 3: Difference between ERAinterim and DFS4.3 downwelling shortwave radiation (mean 1989-2001)

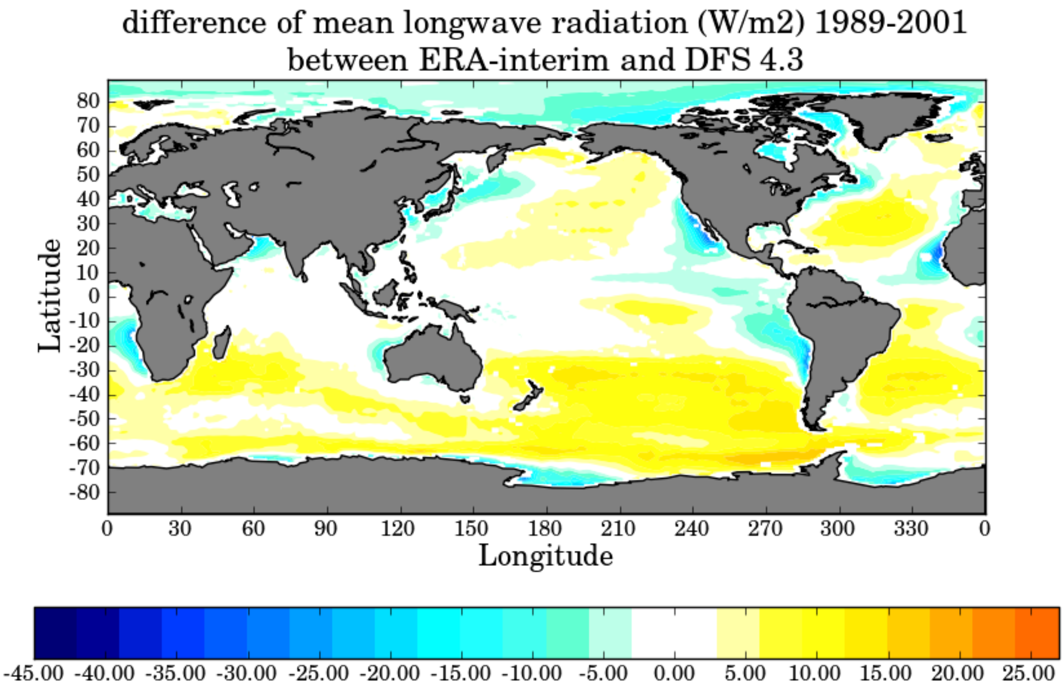

Figure 4: Difference between ERAinterim and DFS4.3 downwelling longwave radiation (mean 1989-2001)

2 Description of the corrections

In this section, we explain the methodology used to correct the various atmospheric variables. When it is necessary, we justify the choice for our method among others. The results of coarse-resolution model (ORCA2) sensitivity simulations are shown to provide validation of the corrections. We will start with turbulent variables (air temperature and humidity and wind speed), then we will describe radiative and freshwater fluxes.

2.1 Air temperature and humidity in the Arctic

Given that the ECMWF reanalysis ERA-interim is much warmer than DFS4.3 in the Arctic (see figure 5), we apply similar corrections on air temperature and humidity at 2 meters than those proposed by L. Brodeau (Ocean Modeling, 2010). Those correction are based on the POLES monthly climatology for air temperature (`http://iabp.apl.washington.edu/data_satemp.html`) and are only done over ice-covered regions, using a monthly climatology of ice-fraction based on SSM/I satellite data. The POLES air temperature and SSM/I ice-cover climatologies have been computed over the period 1979-1998. The method then consists in computing a climatological monthly offset of air temperature between the atmospheric reanalysis and POLES observations. Then a correction based on this offset is applied to the high-frequency fields.

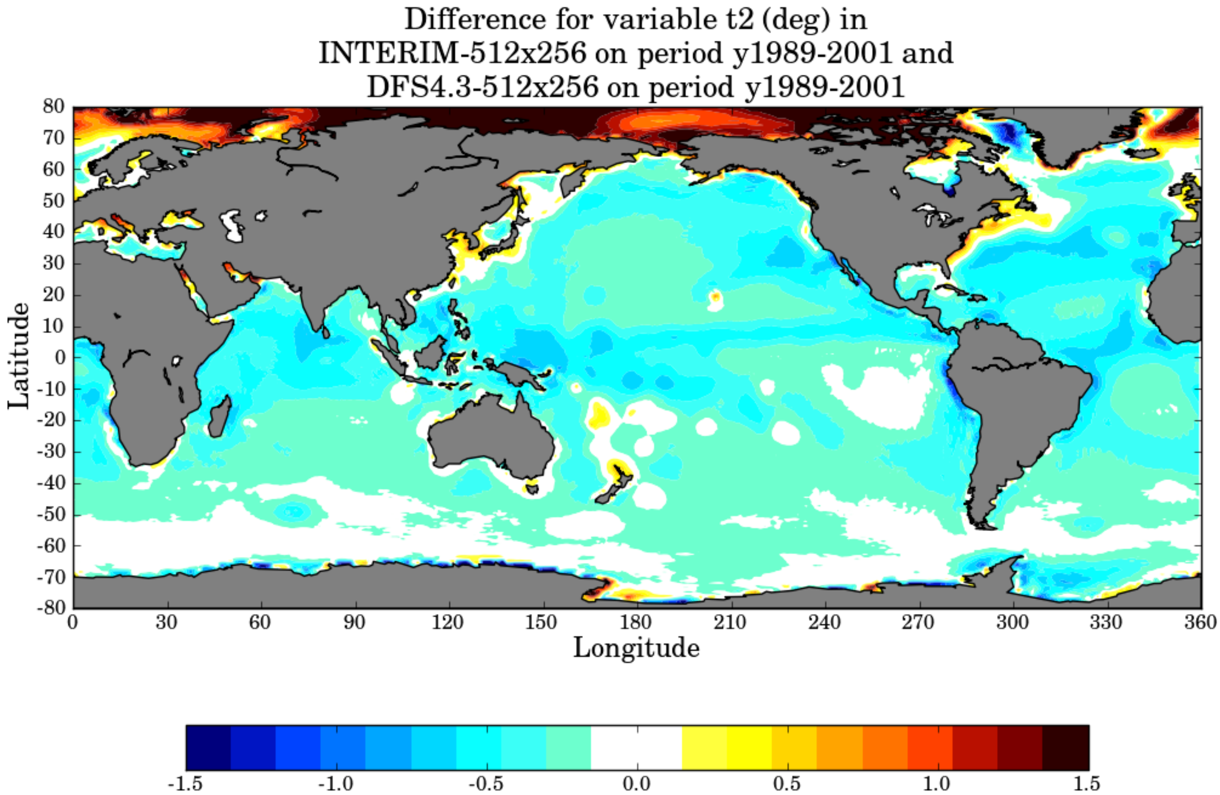

Figure 5: difference in air temperature between ERA-interim and DFS4.3

Figures 6 and 7 show the ice area and extent in respectively march and september in two ORCA246 simulations compared to observations from NSIDC (blue curves). The reference ORCA246 simulation (forced by original ERAinterim) is shown with red curves and the corrected ERAinterim (with only air temperature and humidity corrections in the arctic) is shown with black curves. It appears that the reduction of air temperature gives an overestimation of ice area in winter but a better extent. In summer, there is a major improvement of both ice area and extent. As this modification was already applied to ERA-40 in order to build DFS4.3, it was relevant to reproduce it on ERAinterim to build DFS5. Theses modifications gives good results on ice properties and have a very minor impact of global net heat flux.

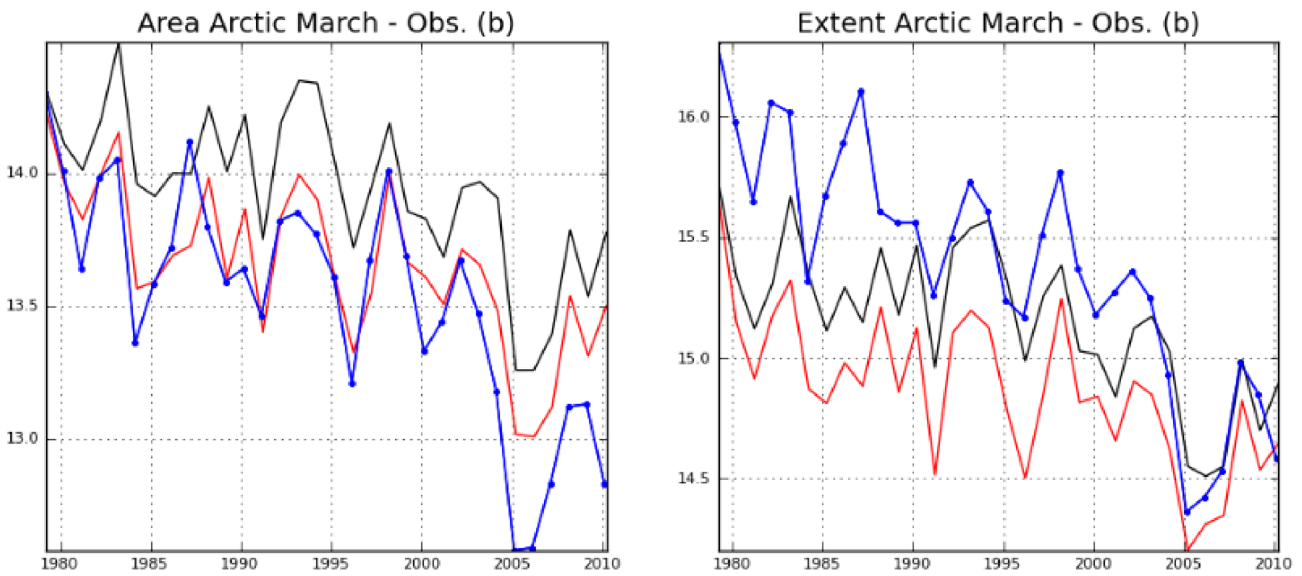

Figure 6: Ice area and extent in march in two ORCA246 simulations forced by original ERAinterim (red) and corrected ERAinterim (black). blue curves are observations from NSIDC

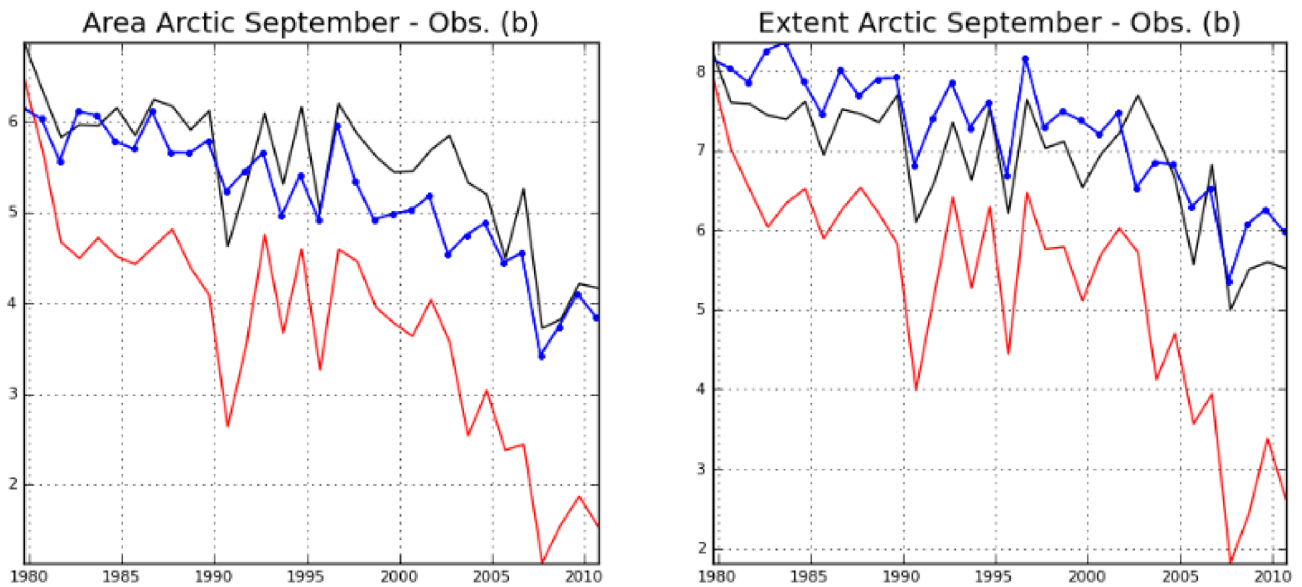

Figure 7: Ice area and extent in september in two ORCA246 simulations forced by original ERAinterim (red) and corrected ERAinterim (black). blue curves are observations from NSIDC

2.2 Wind speed

ERAinterim forced simulations have shown to have weak gyre circulation so it was decided to increase wind speed, which is reasonable given that it is a known flaw of the reanalysis. Figure 8 shows the zonal mean of wind module (time-averaged over the period 2000-2006) in ERAinterim, DFS4.3 and QuikSCAT. The gray shaded area corresponds to uncertainties on QuikSCAT data. Though ERAinterim mean wind module is within the error bars, we clearly see that ERAinterim have weaker values than QuikSCAT almost everywhere. The major discrepancies are found between 40°S and 40°N , which can be as large as 0.8 m/s at the equator. In DFS4.3, ERA-40 winds have been rescaled towards QuikSCAT so that values are obviously closer but still a little less intense than QuikSCAT.

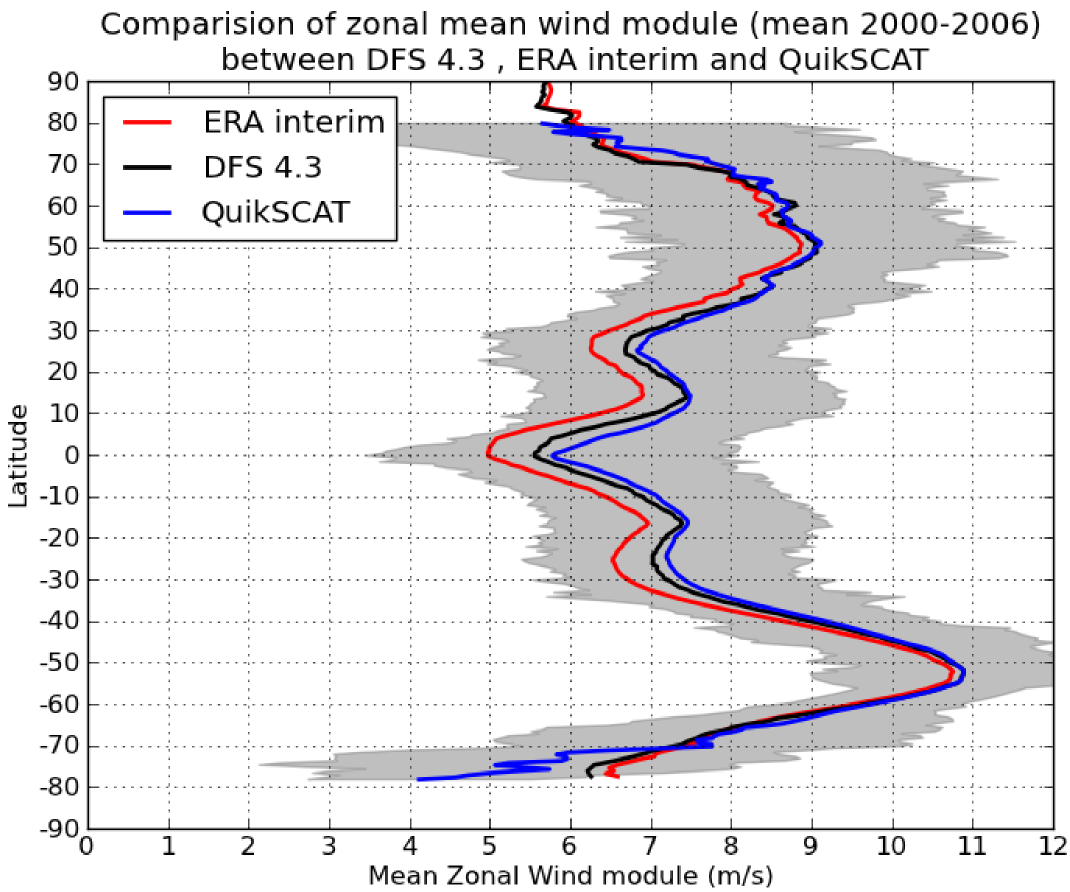

Figure 8: comparison of zonal mean wind module (2000-2006). Gray shaded area corresponds to uncertainties on QuikSCAT.

After various attempts, it has been decided to re-enforce winds by adding a background value based on the QuikSCAT over ERAinterim mean wind module ratio. This solution have been chosen instead of simple multiplication of wind speed by a ratio because it allows to have lower evaporation. Let us define a ratio of QuikSCAT over ERAinterim wind module such as :

$$\alpha = \frac{\frac{1}{T}\sum_i U^i_{QuikSCAT}}{\frac{1}{T}\sum_i U^i_{ERAi}} \tag{1}$$

where T is the 2000-2008 period and U is the wind module at each timestep defined as :

$$U = \sqrt{u_{10}^2 + v_{10}^2} \tag{2}$$

The obtained ratio is somewhat noisy so it is smoothed with a anisotropic box filter. the box size is 14 grid points along the meridional direction and 28 grid points along the zonal direction, which corresponds to a 10° by 20° box. The ratio has been expanded over twice the domain, then filtered and recomposed on the original grid to avoid a discontinuity at 0°W . The maximum correction allowed is 15 percent, there is no correction above of 60°N and below of 60°S and a linear transition is done on 10 gridpoints (about 7° in latitude). In the multiplicative ratio method, the wind speed is rescaled at each timestep by the smoothed ratio α_{sm} :

$$u_{10}^{*} = \alpha_{sm} \times u_{10} \tag{3}$$
$$v_{10}^{*} = \alpha_{sm} \times v_{10} \tag{4}$$

With the background value method, we use the same ratio but we apply it in the following way :

$$u_{10}^{*} = (\alpha_{sm} - 1) * \bar{u}_{10} + u_{10} \tag{5}$$
$$v_{10}^{*} = (\alpha_{sm} - 1) * \bar{v}_{10} + v_{10} \tag{6}$$

As the increase of wind speed leads to enhanced evaporation, multiplication by a ratio will gives a proportional increment of wind speed even in extreme events. This would lead to great evaporation rates which is something we want to prevent in order to keep a reasonable freshwater balance. Figure 9 shows the difference of evaporation between the multiplicative ratio (v1) and background value method (v2). We clearly see that the background value method reduces dramatically evaporation (up to 1 mm/day in the Gulf Stream). Figure 10 shows the global evaporation and net heat flux (averaged over the period 1979-2010) : it confirms reduction of the evaporation when using background value method and also emphasizes the impact on net heat flux.

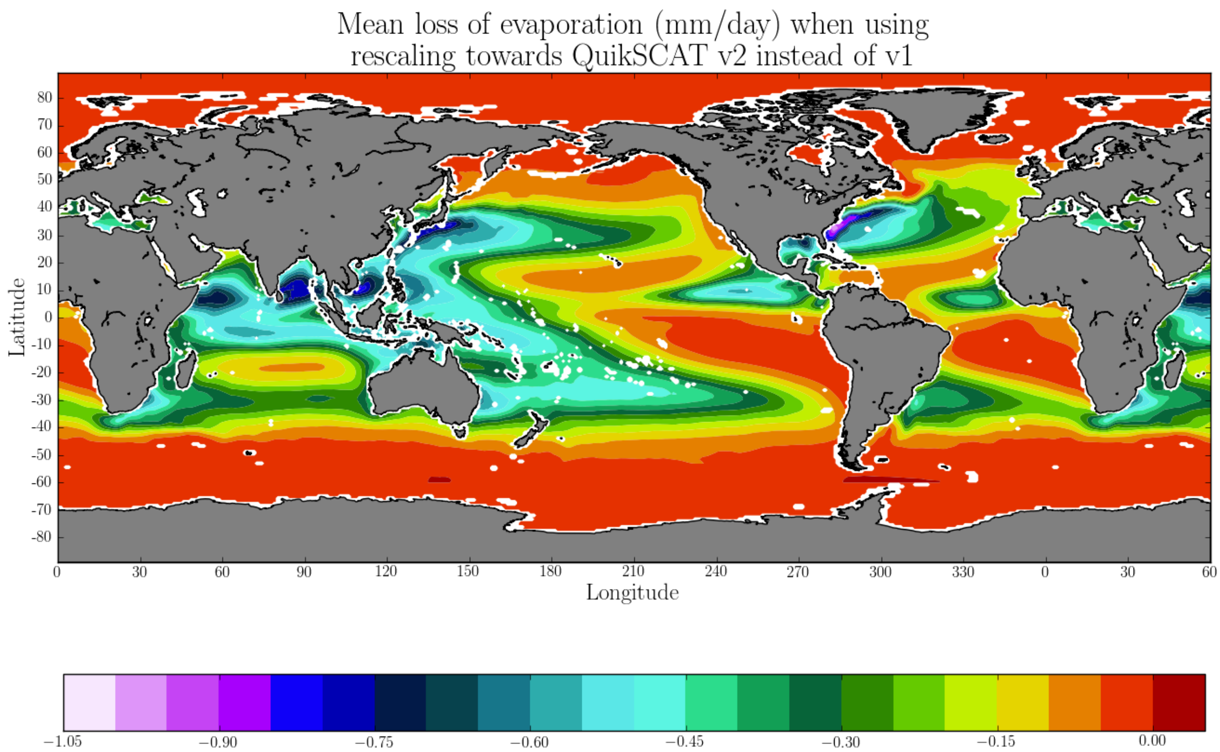

Figure 9: Difference of evaporation between background value method (v2) and multiplicative ratio method (v1). Negative values corresponds to a diminution of evaporation in the background value method compared to multiplicative ratio method.

The v2 method gives an excess evaporation compared to ERAinterim of 0.15 mm/day which is more reasonable than the 0.35 provided by v1 method, given that this evaporation will have to be balanced by more precipitations. Concerning net heat flux, v1 provides a dramatic cooling of the ocean whereas v2 is more balanced. As radiative fluxes will also be slightly reduced, net heat flux in v1 is already too low.

	Evaporation (mm/day)	Net Heat Flux (W/m2)
ERAinterim	3.7	5.34
ERAinterim QS v1	4.05	-5.65
ERAinterim QS v2	3.85	0.83

Figure 10: Global mean evaporation and net heat flux (1979-2010)

Finally, to limit evaporation and cooling, it has been decided to apply only 80 percent of the correction so that the wind speed at 10 meters of DFS5.1 are given by :

$$u_{10}^{*} = 0.8 \times (\alpha_{sm} - 1) \times \bar{u}_{10} + u_{10} \tag{7}$$
$$v_{10}^{*} = 0.8 \times (\alpha_{sm} - 1) \times \bar{v}_{10} + v_{10} \tag{8}$$

Figure 11 shows the smoothed multiplicative ratio α_{sm} used in the computations. The augmentation of wind speed is maximum at low latitudes and is also important near the Gulf Stream and Kuroshio. The correction brings 0.5 to 1 Sv increase of the Florida-Bahamas transport in ORCA2, while being still very weak compared to observations due to the model viscosity. The eddy-permitting models are expected to show the similar behavior but with stronger values. No corrections are applied below 60°S and weak corrections are done south of 50°S . The methodology used do not bring additional trend to the signal in order not to affect SAM related studies.

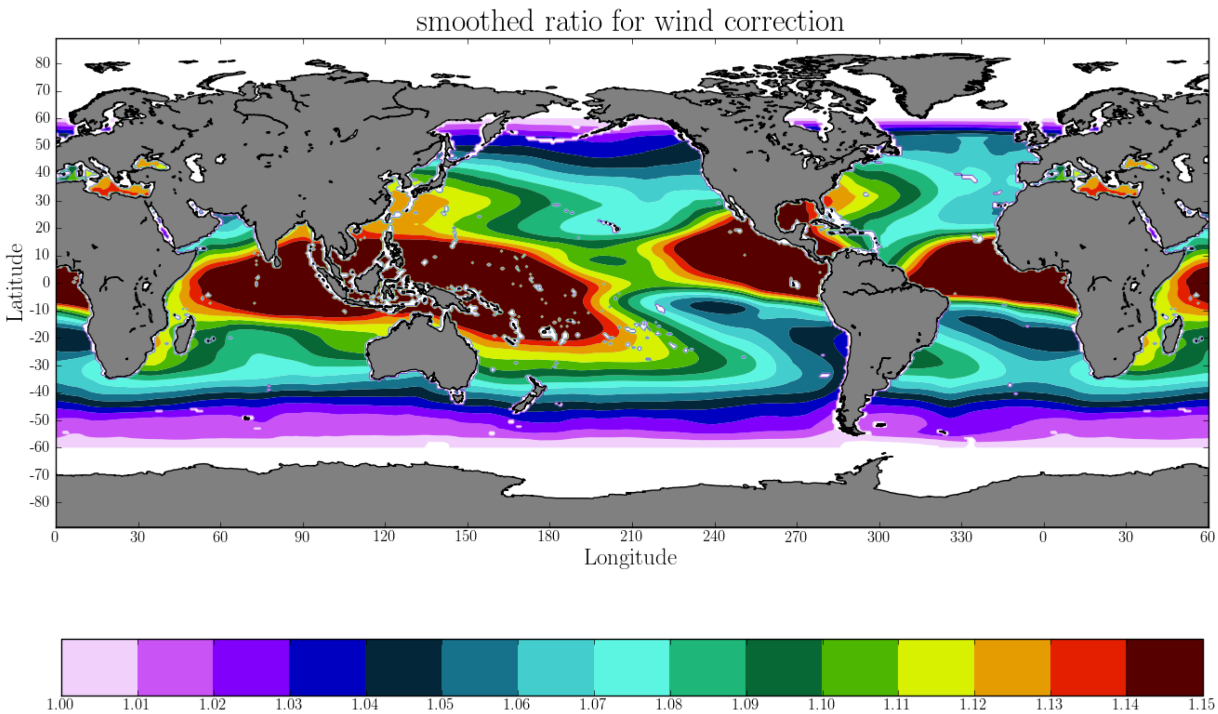

Figure 11: Multiplicative ratio used for wind speed enhancement

2.3 Radiative fluxes

Achieving a good cloud cover representation in atmospheric model is a very tough task as it requires correctly resolved dynamics, as well as humidity and aerosols concentration in the air parcel. This cloud cover will then impact radiative transfer model which ultimately provides the downwelling shortwave and longwave radiation to the ocean model. Compared to satellite products (such as Gewex or ISCCP), it appears that ERAinterim overestimates shortwave radiation and underestimates longwave radiation. It is likely that the errors in cloud representation in ERAinterim consists in a lack a cloud cover, thus leading to the observed biases in the radiative fluxes. Therefore it has been decided to reduce shortwave radiation and increase slightly longwave radiation, using DFS4.3 (which comes from ISCCP satellite data) as our reference.

Due to seasonality, the only available method is obviously the multiplicative ratio. We choose to correct shortwave only when the difference between ERAinterim and DFS4.3, averaged on the period 1984-2006, is superior to 10 W/m2. Longwave radiation is also corrected when difference between ERAinterim and DFS4.3, averaged on the period 1984-2006, is inferior to -2.5 W/m2.

We compute the ratios of ERAinterim over DFS4.3 for both shortwave and longwave radiation, apply drowning to avoid land values and then smooth them using a gaussian filter. Then some masking is applied to remove correction in the high latitudes and closed seas (hudson bay, med and red sea, persian gulf,...). Finally, corrected fields are obtained by simple multiplication of each ERAinterim radiative field by those ratios shown in figures 12 and 13.

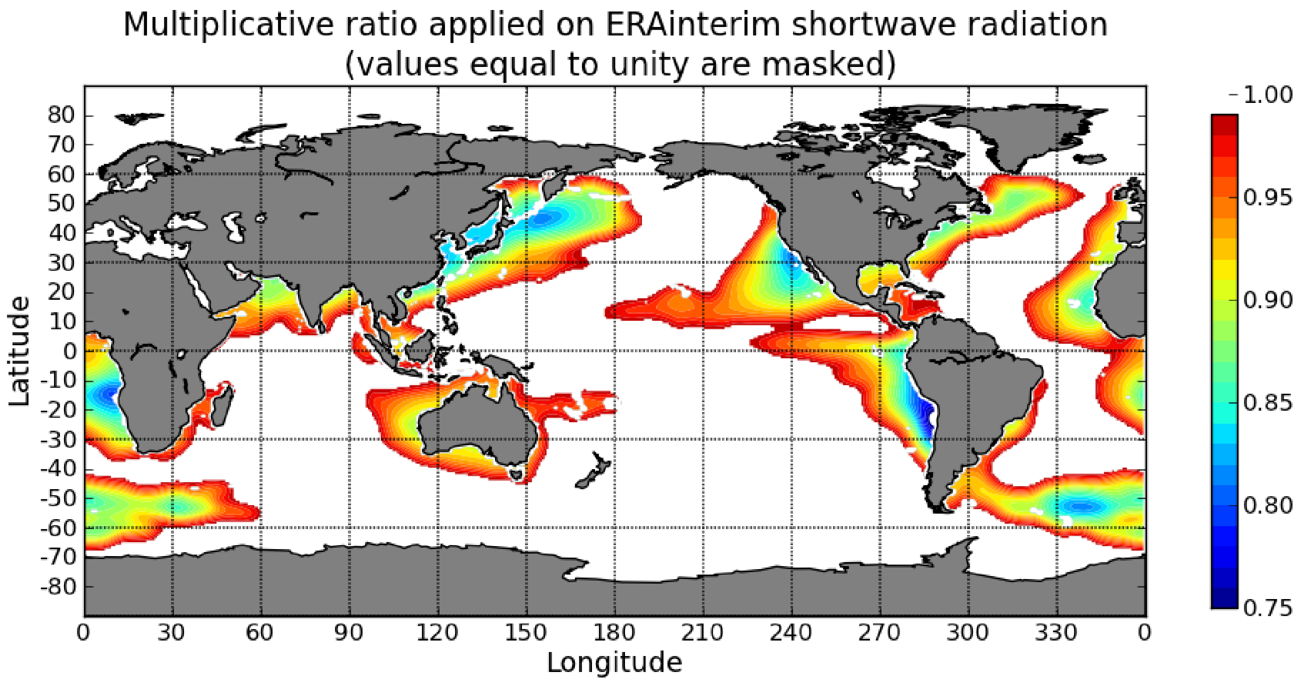

Figure 12: Multiplicative ratio applied to ERAinterim shortwave radiation

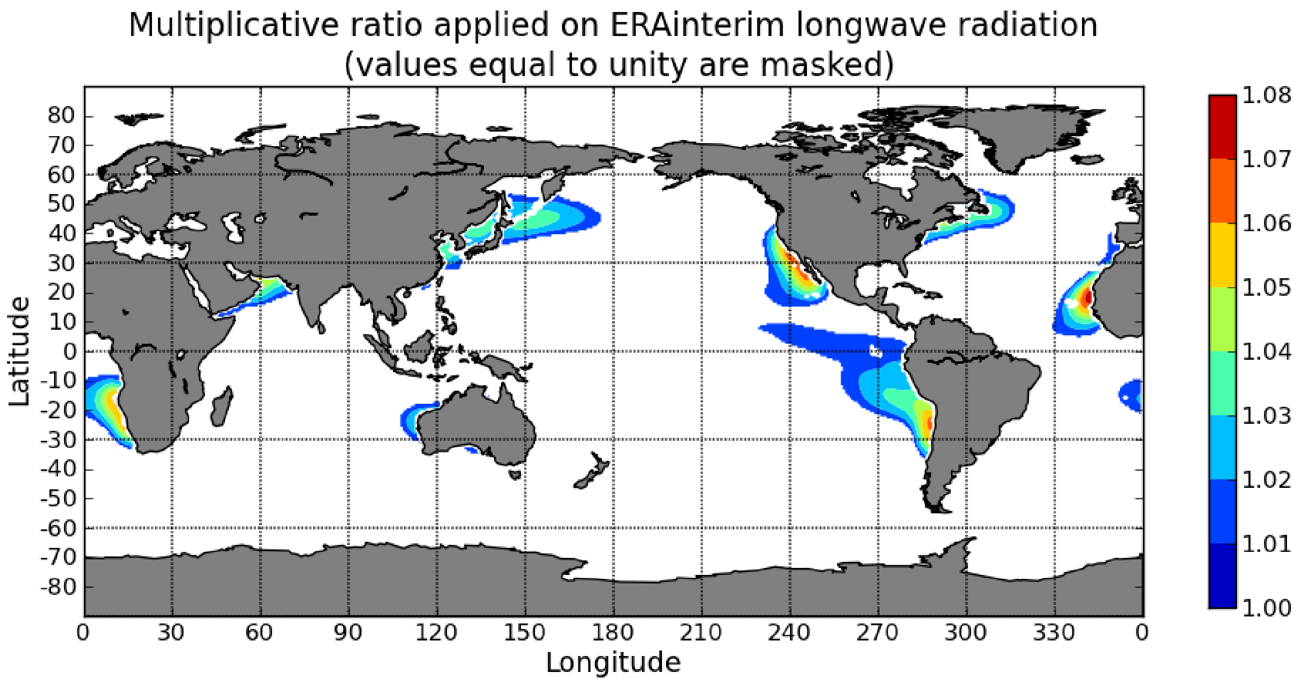

Figure 13: Multiplicative ratio applied to ERAinterim longwave radiation

2.4 Precipitations

Regarding precipitations, various modifications have been performed : the trends have been removed and the corrections proposed by Storto et al. (2010) have been applied on the detrended fields. Figure 15 shows the globally averaged precipitation in ERAinterim as a function of time. It exhibits large variations which act to modify strongly E-P throughout time. The globally averaged E-P in ERAinterim is close to 0.4 mm/day from 1979 to 1992 then gradually rise to 0.8 mm/day in 1998 then oscillates around 0.7 for the rest of the period. Those discrepancies are likely to induce large-scale salinity drift in ocean models. Given that uncertainties on precipitations is quite large, poor confidence should be given to the trends. Thus, it has been decided to detrend the precipitations which helps to stabilize the freshwater budget in time. The resulting E-P have a much lower trend which results from the positive trend in evaporation.

The detrending process was motivated by the inaccuracy of precipitation trend in ERA-interim compared to GPCP satellite product. Figure 14 (adapted from Dee et al., Quart. J. R. Meteorol. Soc. 2011) shows the precipitation trends in ERA-interim are not comparable to observations and might be due to to the variational bias correction.

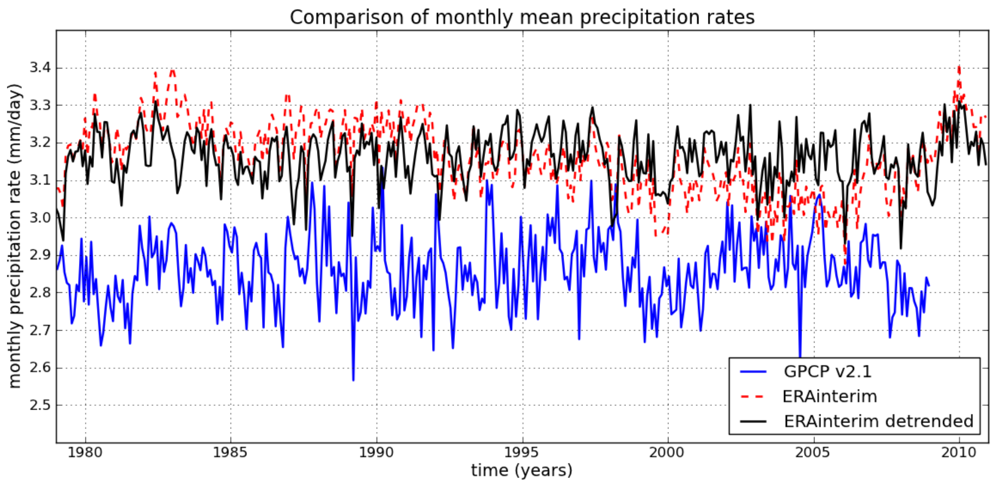

Figure 14: Monthly averaged precipitation estimates for 1979-2010 from ERA-Interim (red), ERA-Interim detrended (black), and GPCP (blue), averaged for all ocean locations. Adapted from Dee et al., Quart. J. R. Meteorol. Soc. 2011

The methodology used lies in separating the full ERAinterim period into 3 periods (1979-1991, 1992-2004, 2005-2010), which exhibits respectively positive, negative then positive again trends. For each period, we detrend the precipitations on each point using the significative trend (two-tailed t-test) computed over this period. Figure 16 shows the result of detrending : we clearly see the steps in 1992 and 2005 and that the time-averaged mean has decreased (from 3.16 mm/day to 3.14 mm/day). Then each period is rescaled to the original 1979-2010 mean of 3.16 mm/day to avoid steps and conserve total precipitations over the full ERAinterim period. Figure 17 shows the result of the rescaling.

Figure 18 shows the drift in 3d-integrated salinity and the level-integrated salinity profile for two ORCA246 simulations : the reference experiment (red curve) uses original ERAinterim forcing and the sensitivity (black curve) uses ERAinterim with detrended precipitations (but no other modifications). Whereas ERAinterim-forced simulation has a very stable salinity drift, detrending provides a negative salinity drift in the sensitivity experiment. However this drift is very small compared to what would be obtained in a simulation with no SSS restoring. The detrended precipitations also tend to limit the positive salinity drift at a 100 meters depth. From these results, it has been shown that detrending do not have negative impact on simulations, although positive impact is small.

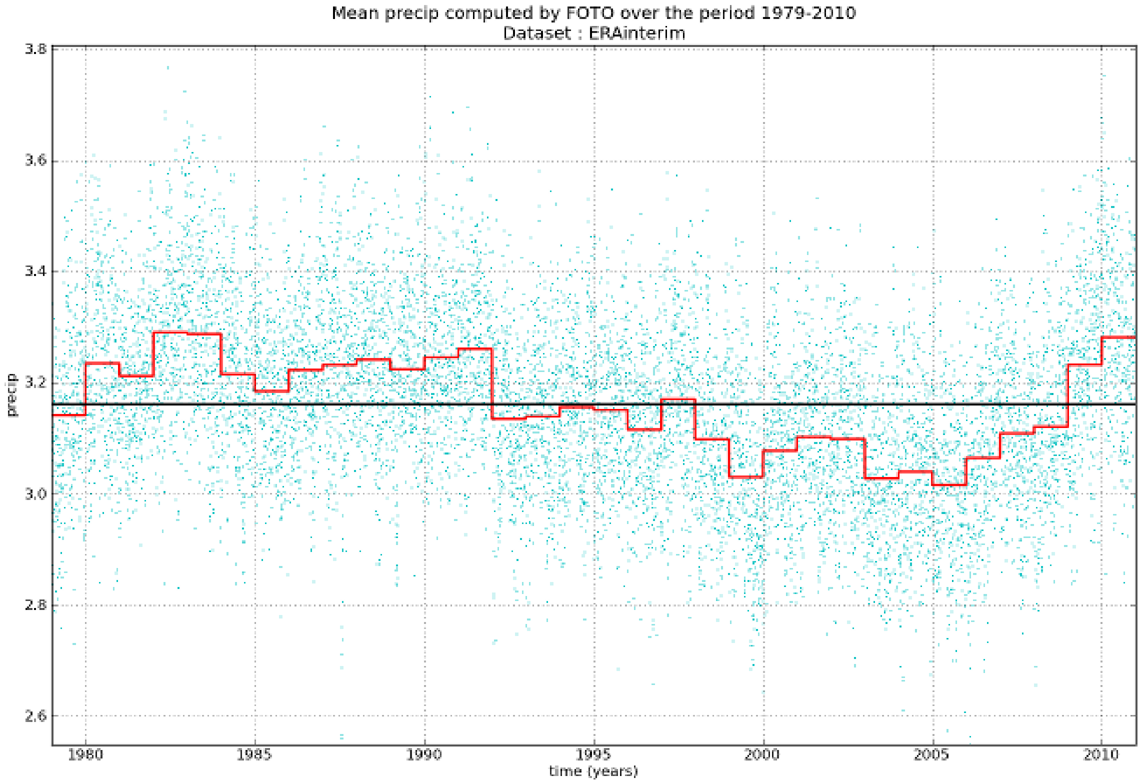

Figure 15: Globally averaged precipitation in ERAinterim

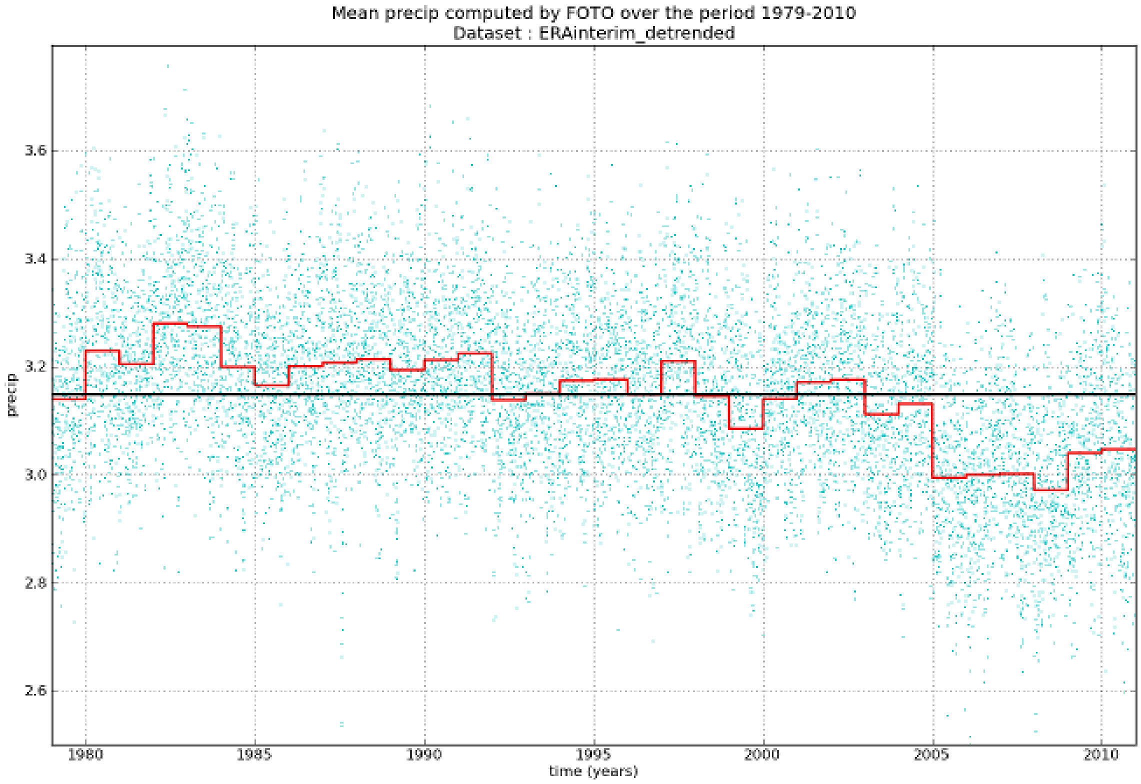

Figure 16: Globally averaged detrended precipitation in ERAinterim. Notice the steps in 1992 and 2005 due to detrending and the mean value (black curve) is lower than in ERAinterim

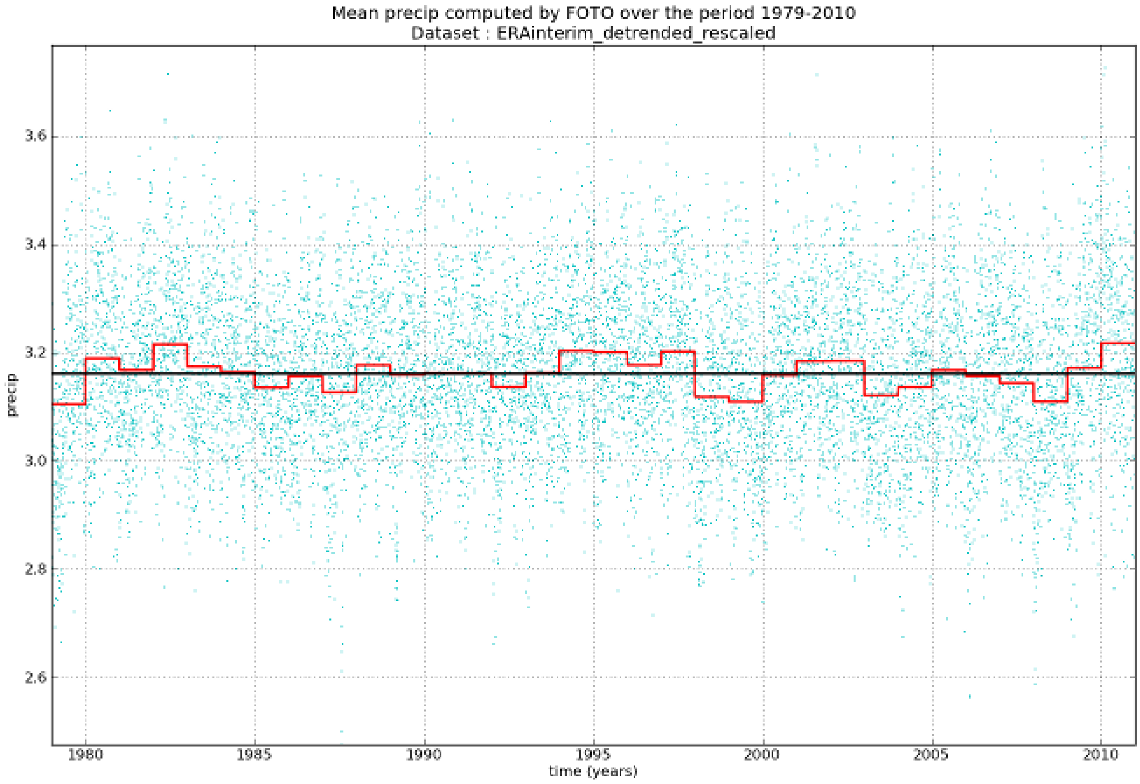

Figure 17: Globally averaged detrended and rescaled precipitation in ERAinterim. There is no discontinuities in 1992 and 2005 and the mean is back to the original value

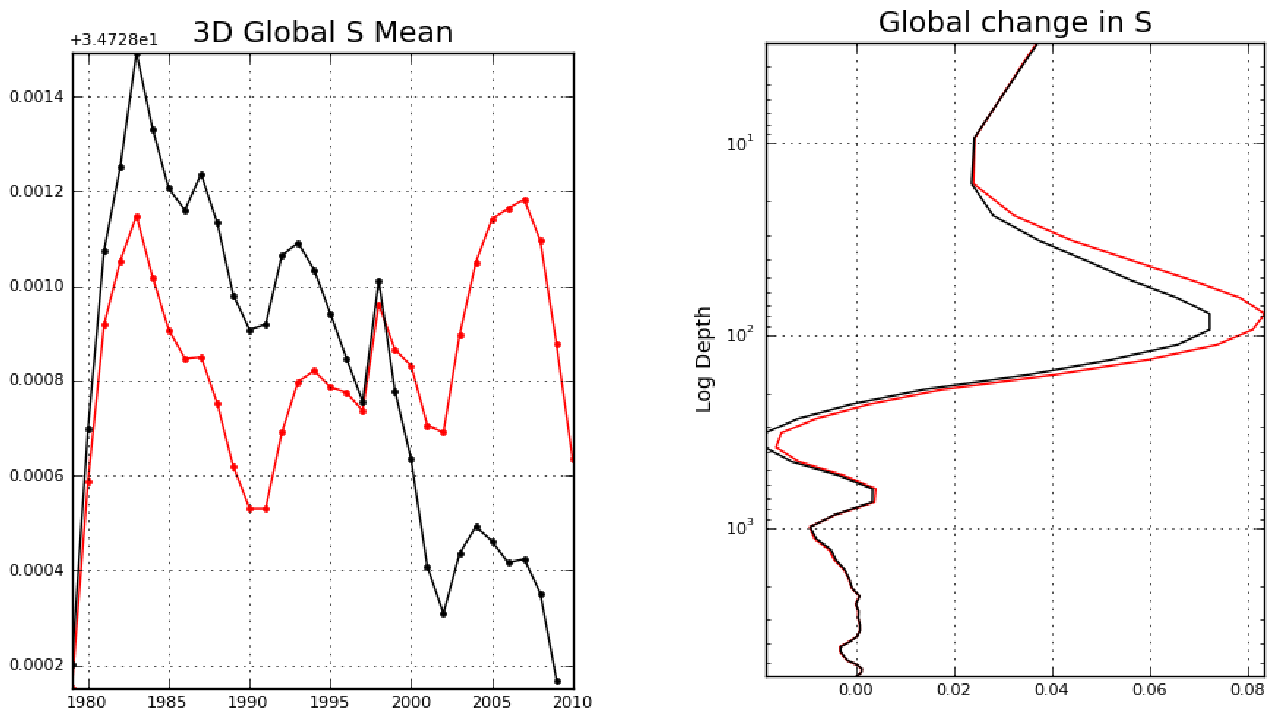

Figure 18: Salinity trends in ORCA246 experiments : 3d-integrated value *(left)* and level-integrated profile of year 2010, after 30 years of run *(right)*. Red curve is the original ERAinterim, black curve is ERAinterim with detrended precipitations.

Finally, we have applied the method of Storto et al. to the detrended precipitations with some modifications. The method of Storto was designed to work online (in sbcblk_core module) in the case of an ORCA025 simulation. As our purpose is to provide a standalone corrected forcing set on the native grid, we adapted the Storto code to run it offline. However interpolation to ORCA025 was needed to apply the correction, thus fields have been interpolated twice : from native to ORCA025 grid before correction then from ORCA025 to native grid after correction. Storto provides a monthly correction field to apply on precipitations based on PMWC (Passive Microwave Water Cycle) which has a 0.25° spatial resolution and monthly frequency. Whereas Storto suggests to interpolate in time this corrective term, we found it inappropriate because what we consider important is to conserve the total amount of added (or retrieved) precipitations over the month.

Figure 19 shows the correction provided by Storto et al. on original ERAinterim (not detrended). Though the obtained corrected field (after detrending) will be slightly different (see next section), this illustrates the main effects of this correction. The correction decrease mean precipitation in the western tropical atlantic and pacific which will allow to minimize fresh biases found with ERAinterim in these regions. Precipitations are also stronger in northern hemisphere subtropical gyres with a strong increase along canadian east coast which is more surprising.

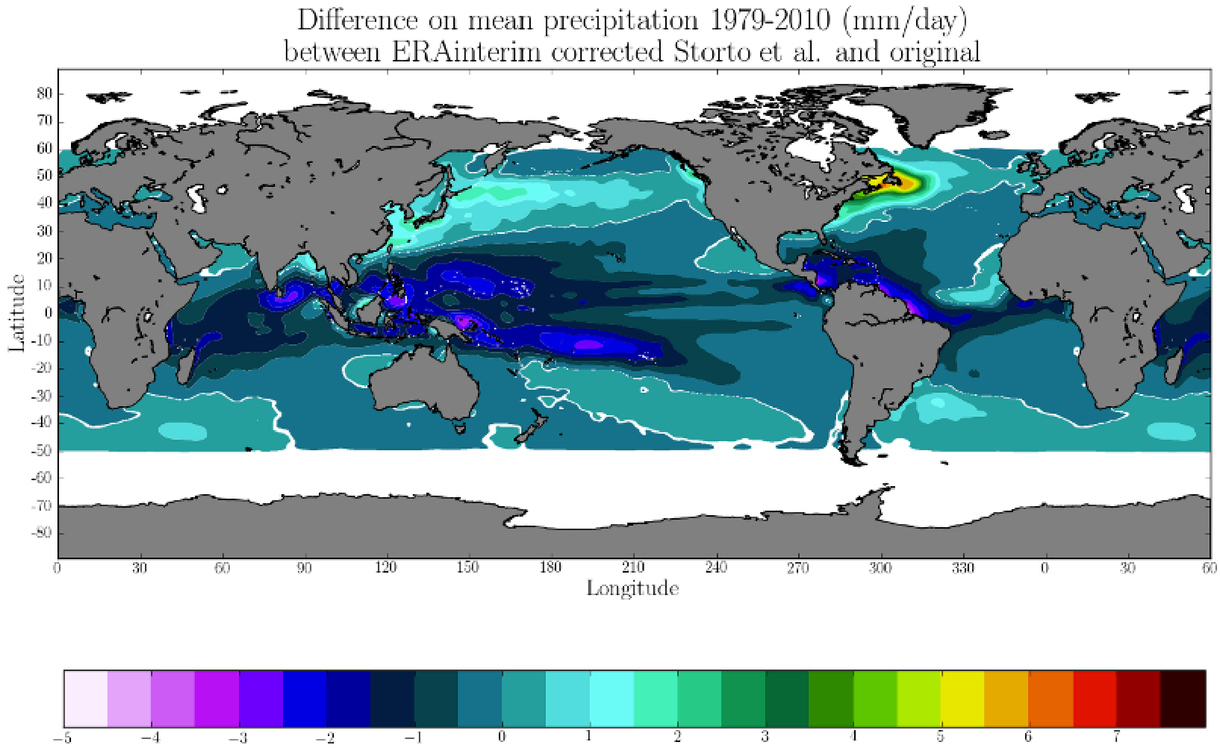

Figure 19: Difference between mean (1979-2010) precipitations in ERA-interim corrected by Storto and original ERAinterim

In the next section, we show the results of all the modifications performed on ERA-interim. We focus on the differences between DFS5.1 and ERA-interim and provide informations mostly on the climatological mean and interannual variations. This is presented as an atlas to give the essential information about DFS5.1. As mentioned is the introduction, more exhaustive diagnostics are available in FARC reports (ask the authors).

3 Atlas of comparisons with ERA-interim

3.1 Temperature at 2m

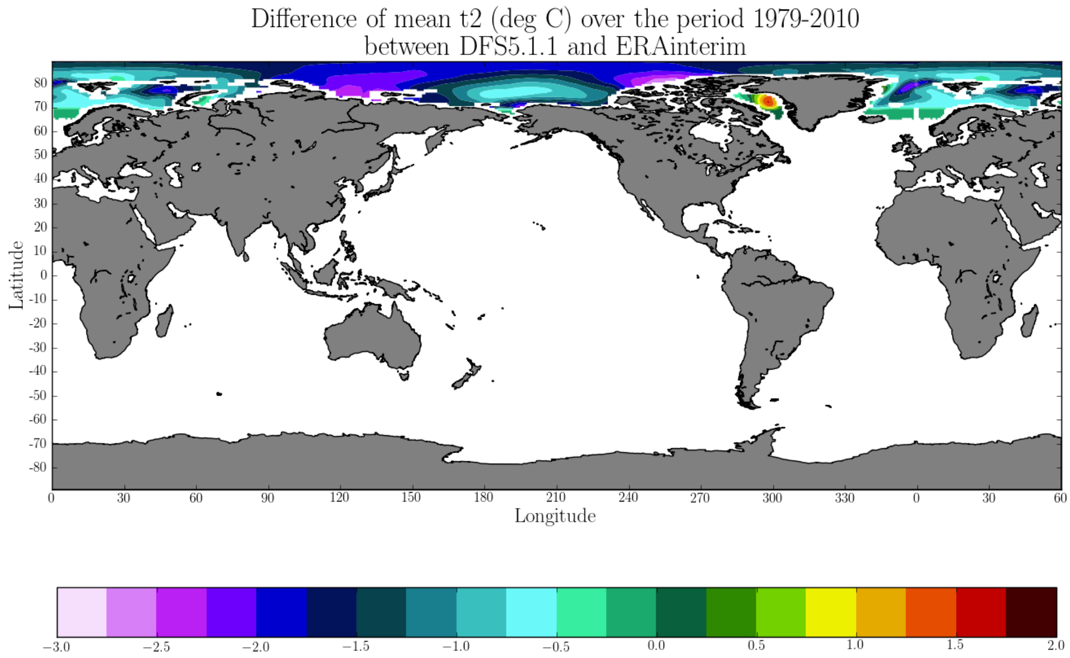

Figure 20: Difference between mean (1979-2010) t2 between DFS5.1 and original ERAinterim

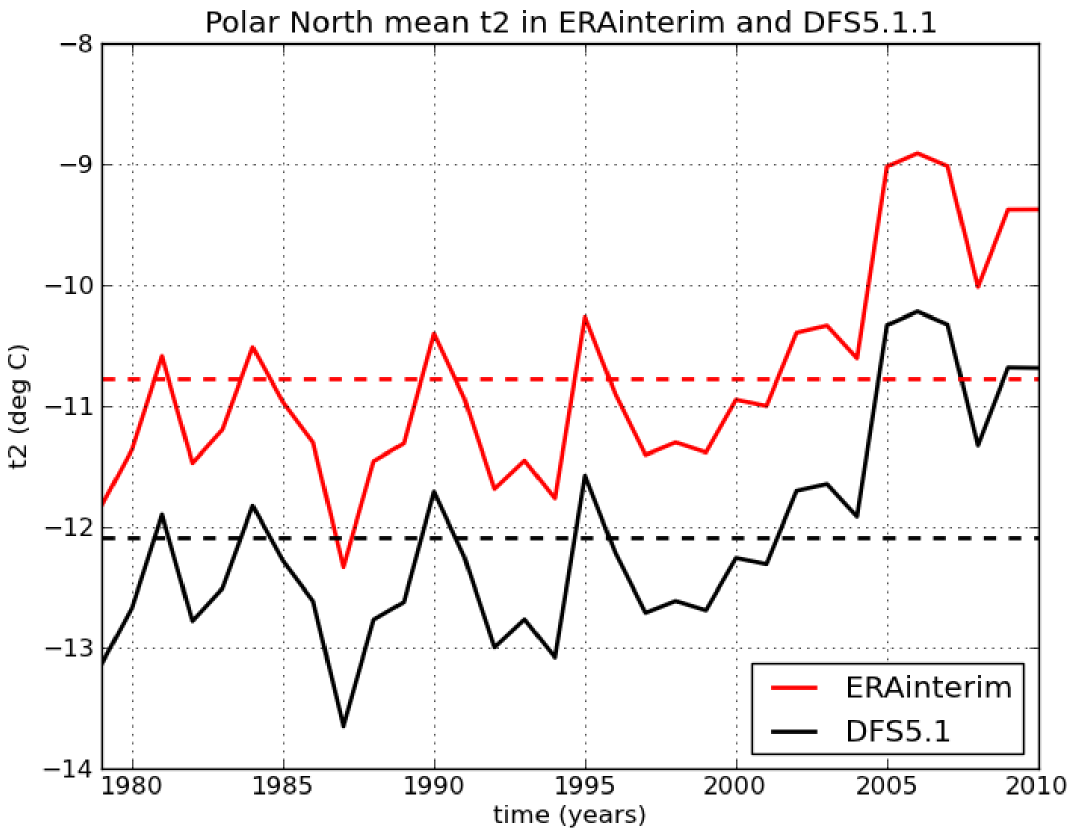

Figure 21: timeserie of annual mean t2 (70 to 90°N only) in ERAinterim and DFS5.1

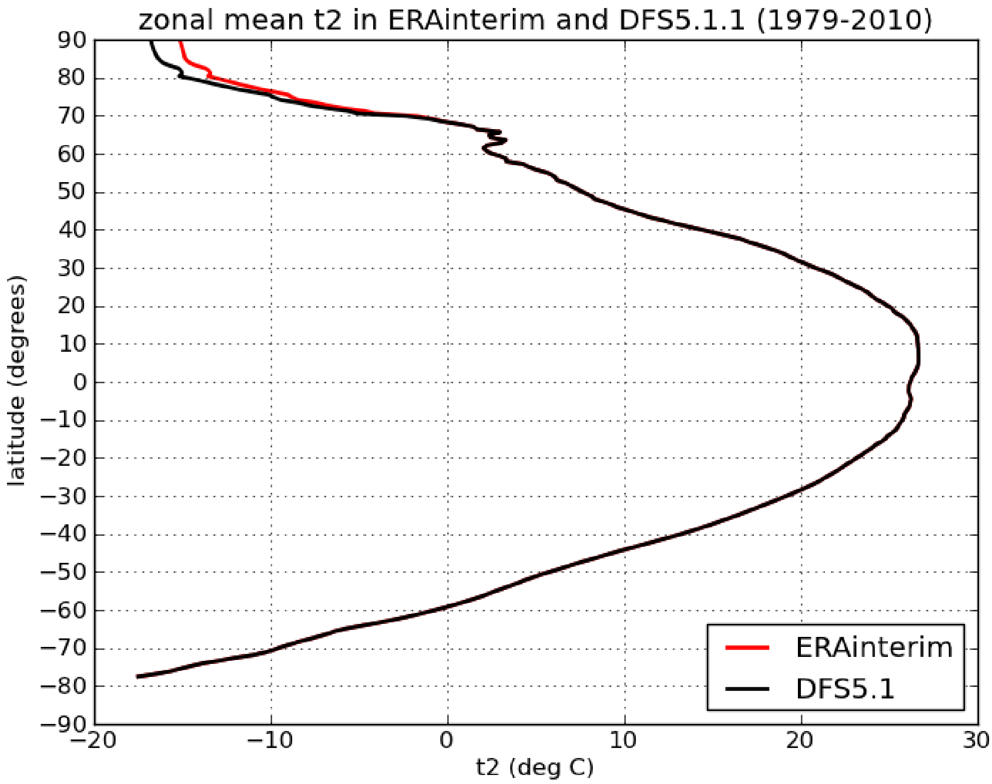

Figure 22: Zonal mean (1979-2010) t2 in DFS5.1 and original ERAinterim

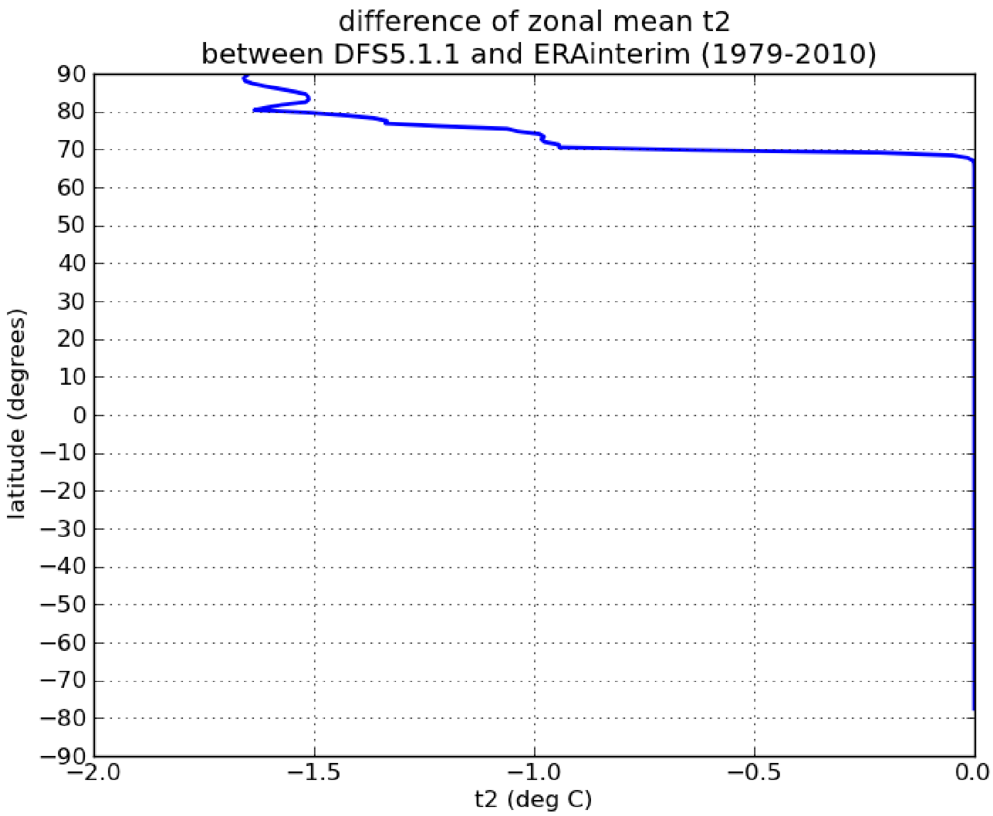

Figure 23: Difference between zonal mean (1979-2010) t2 between DFS5.1 and original ERAinterim

3.2 Humidity at 2m

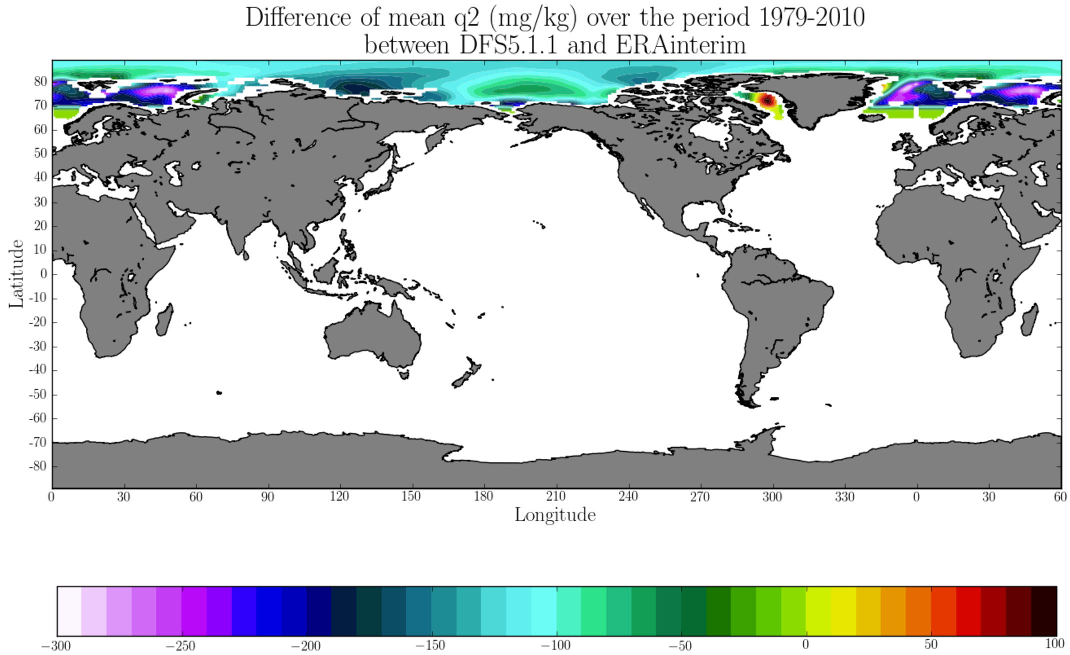

Figure 24: Difference between mean (1979-2010) q2 between DFS5.1 and original ERAinterim

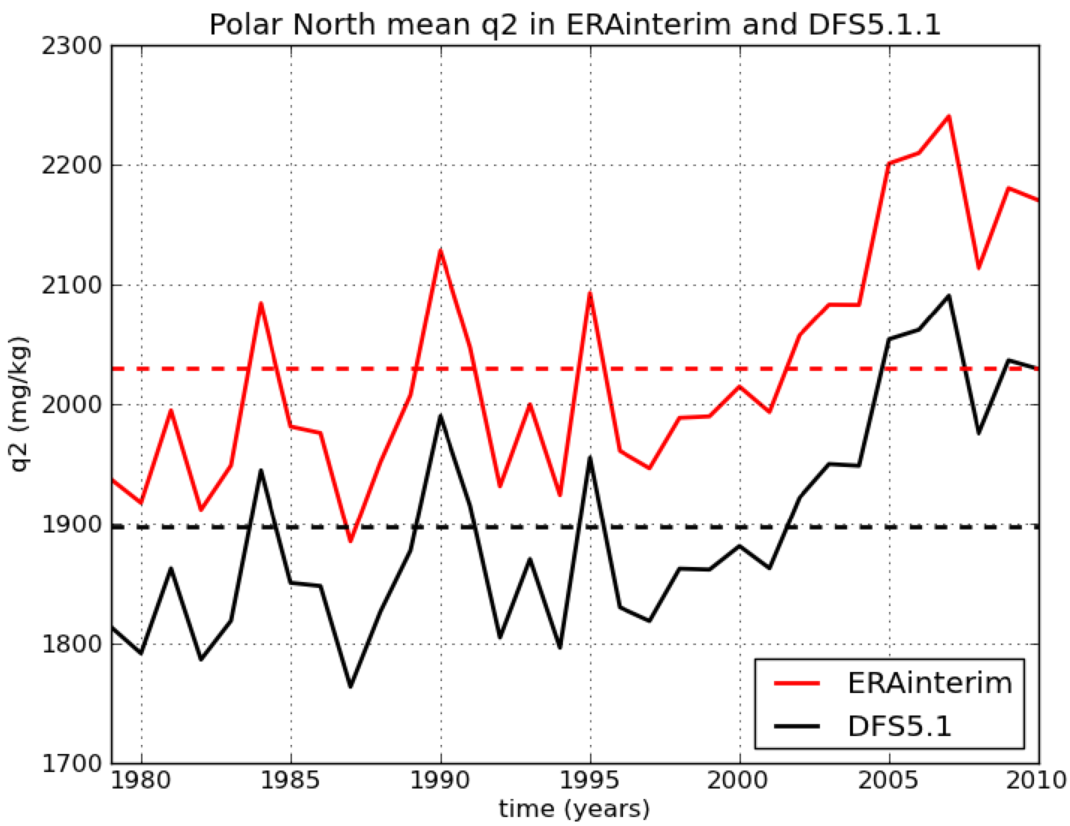

Figure 25: timeserie of annual mean q2 (70 to 90°N only) in ERAinterim and DFS5.1

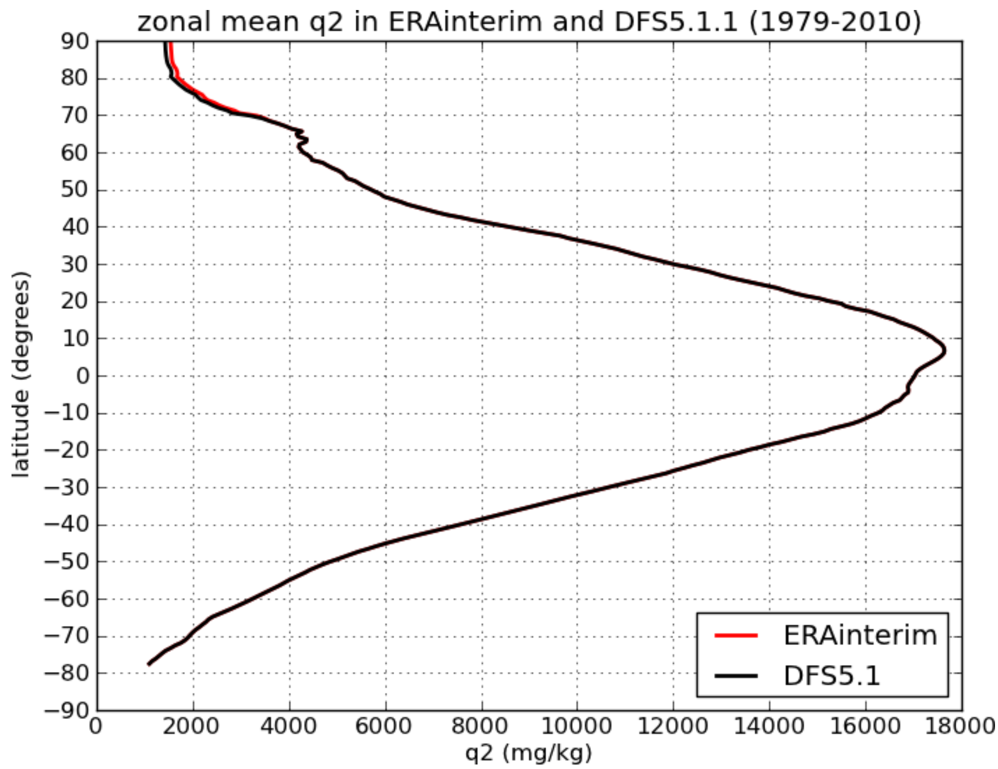

Figure 26: Zonal mean (1979-2010) q2 in DFS5.1 and original ERAinterim

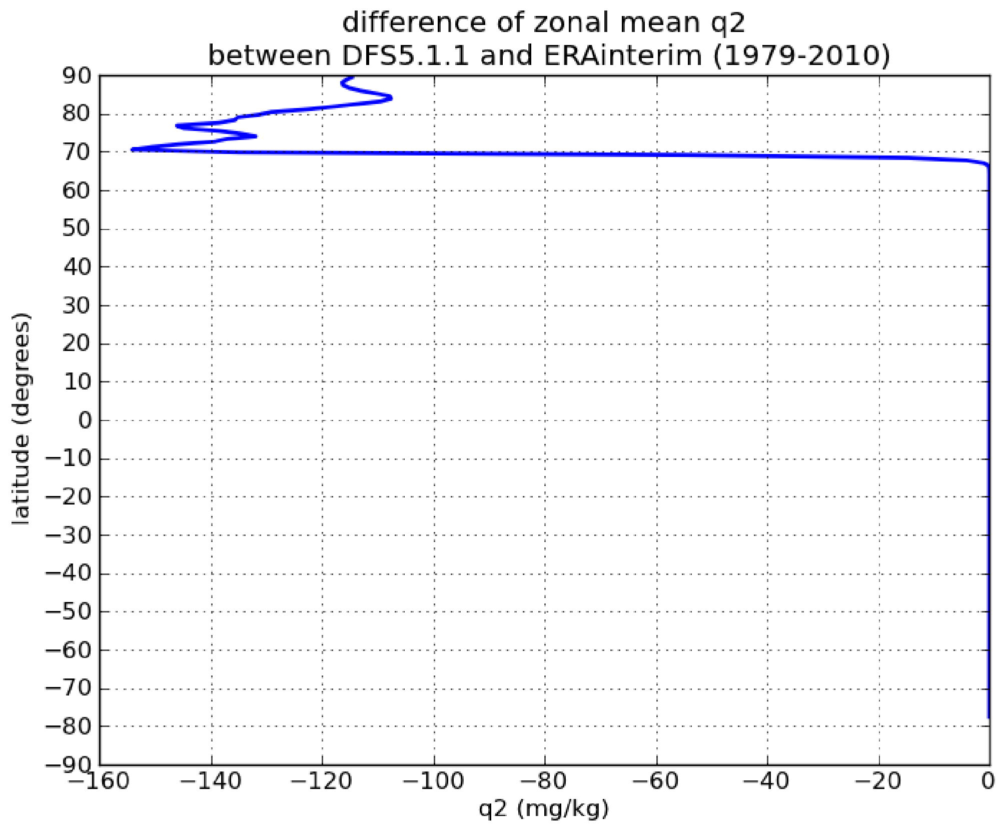

Figure 27: Difference between zonal mean (1979-2010) q2 between DFS5.1 and original ERAinterim

3.3 Zonal wind at 10m

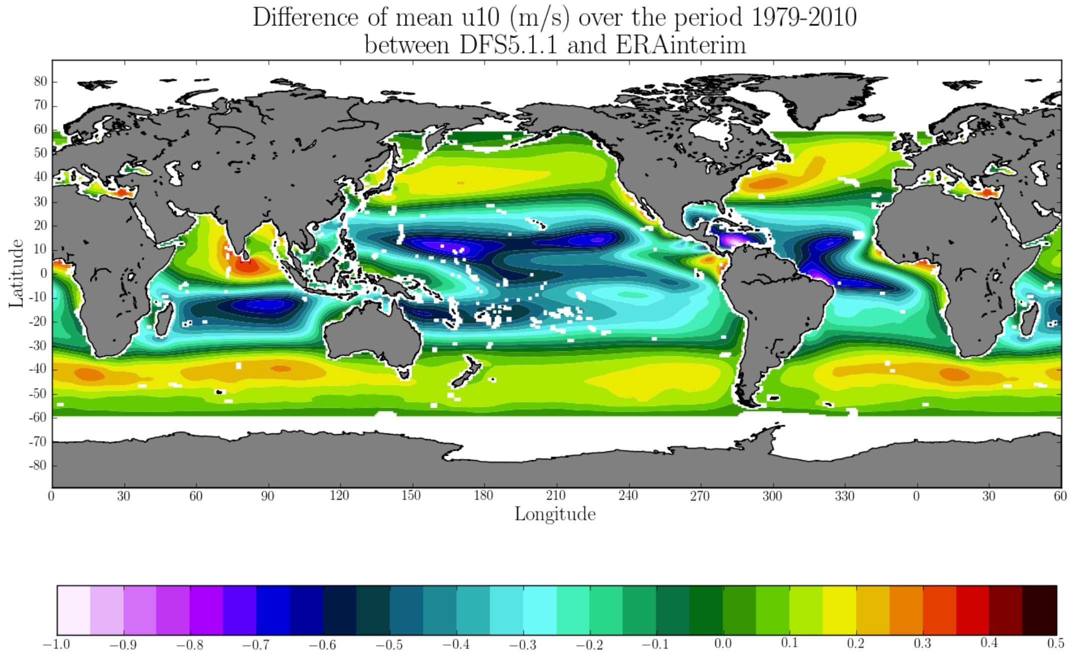

Figure 28: Difference between mean (1979-2010) u10 between DFS5.1 and original ERAinterim

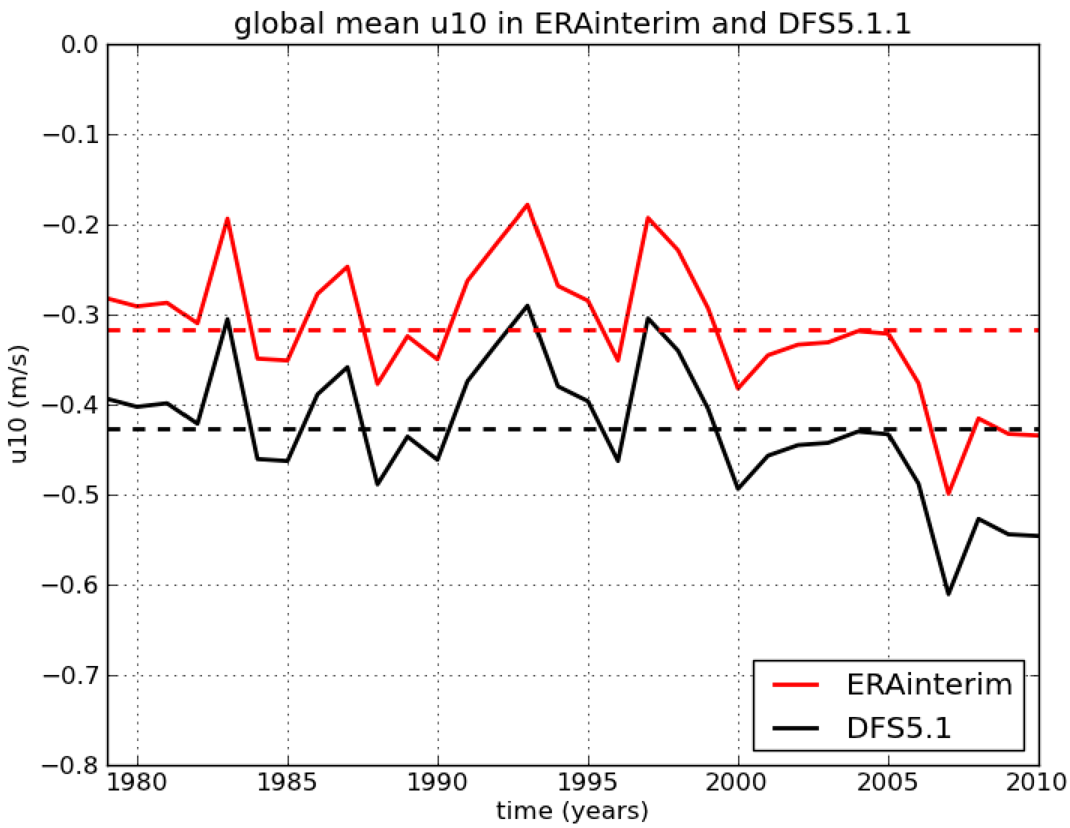

Figure 29: timeserie of annual mean u10 (global) in ERAinterim and DFS5.1. Negative wind speed means eastward, hence absolute wind speed is greater in DFS5.1.

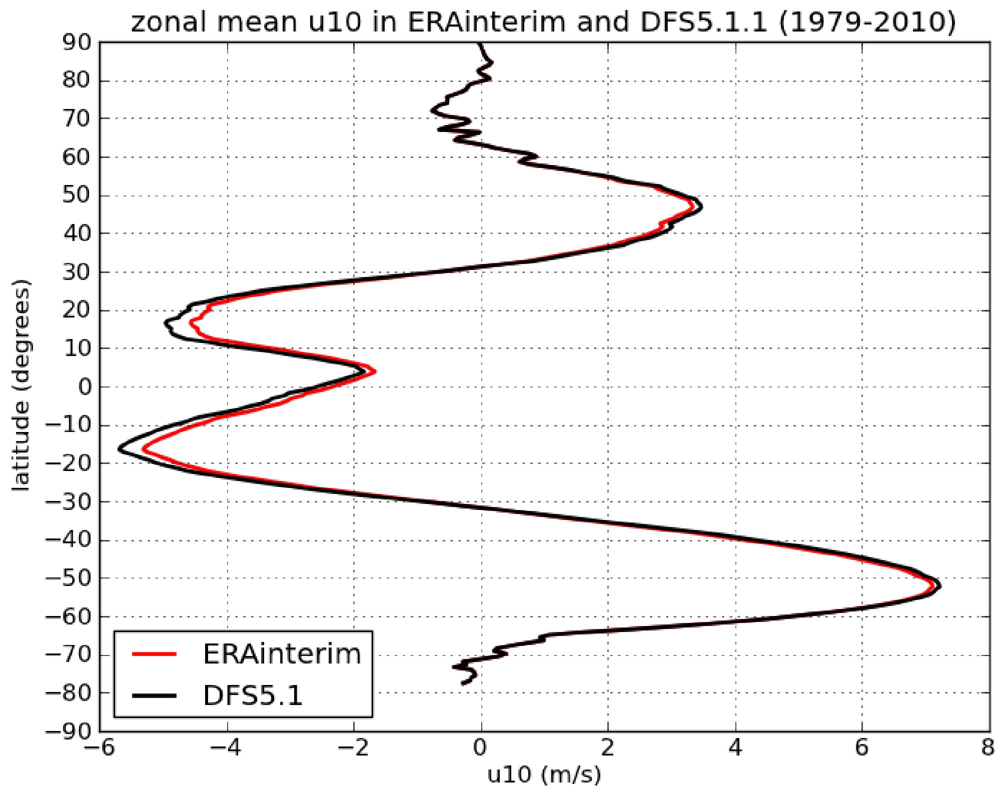

Figure 30: Zonal mean (1979-2010) u10 in DFS5.1 and original ERAinterim

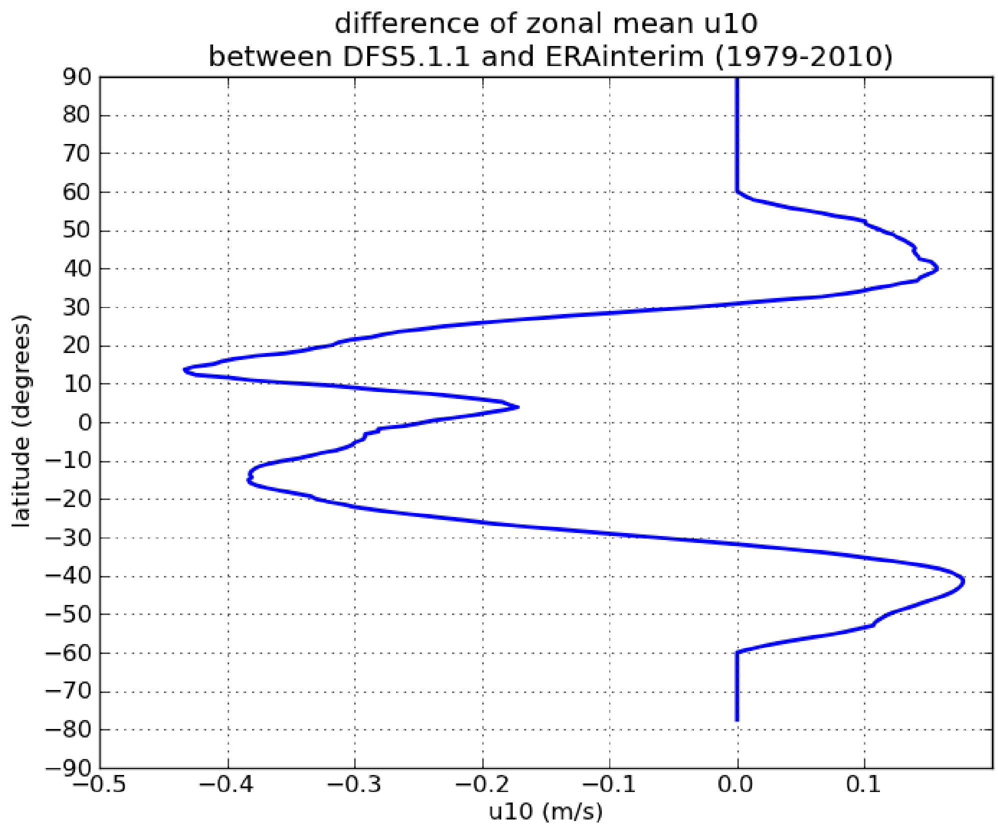

Figure 31: Difference between zonal mean (1979-2010) u10 between DFS5.1 and original ERAinterim

3.4 Meridional wind at 10m

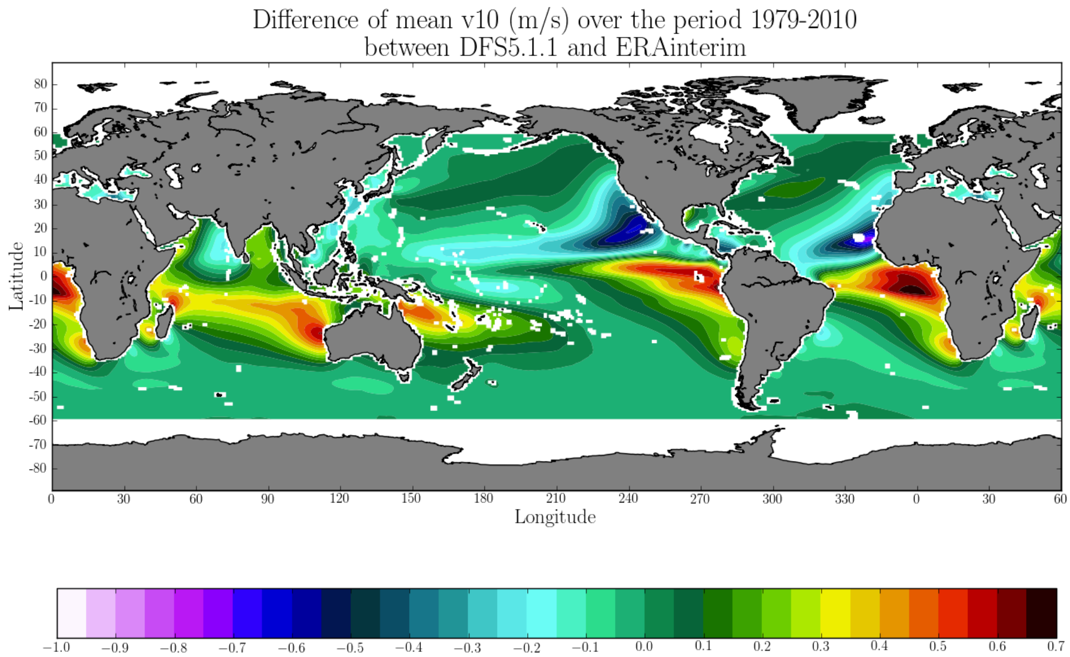

Figure 32: Difference between mean (1979-2010) v10 between DFS5.1 and original ERAinterim

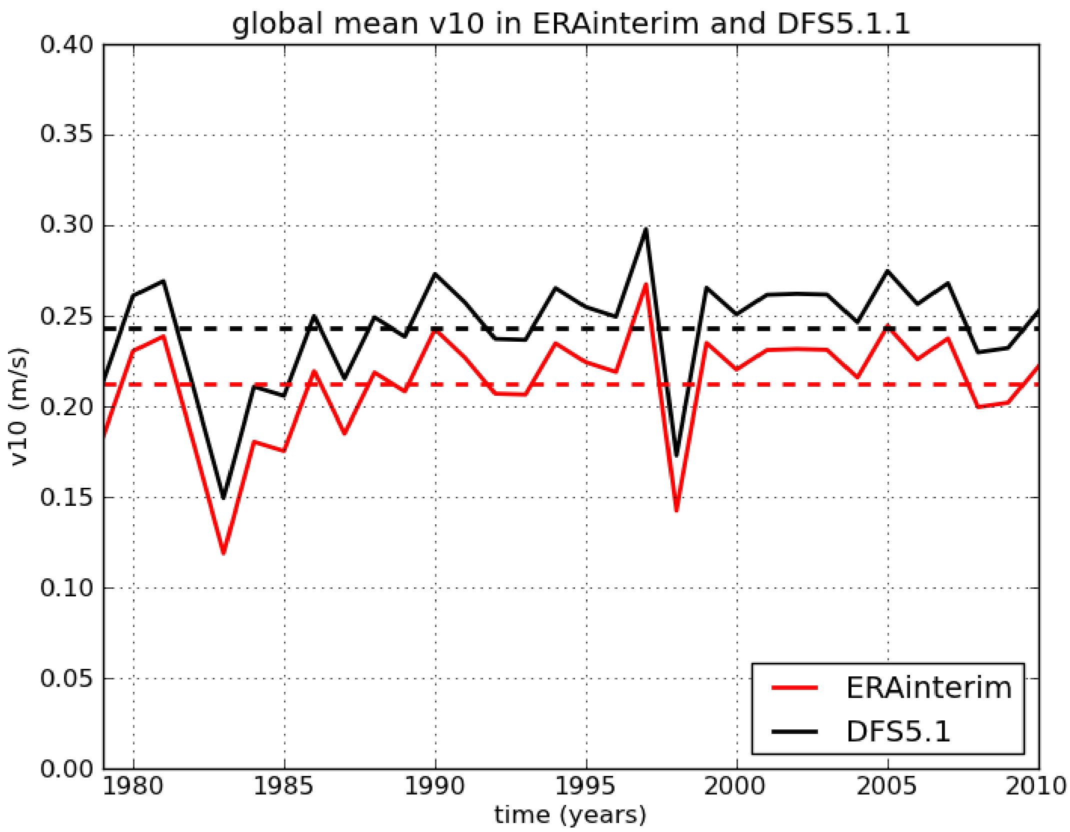

Figure 33: timeserie of annual mean v10 (global) in ERAinterim and DFS5.1

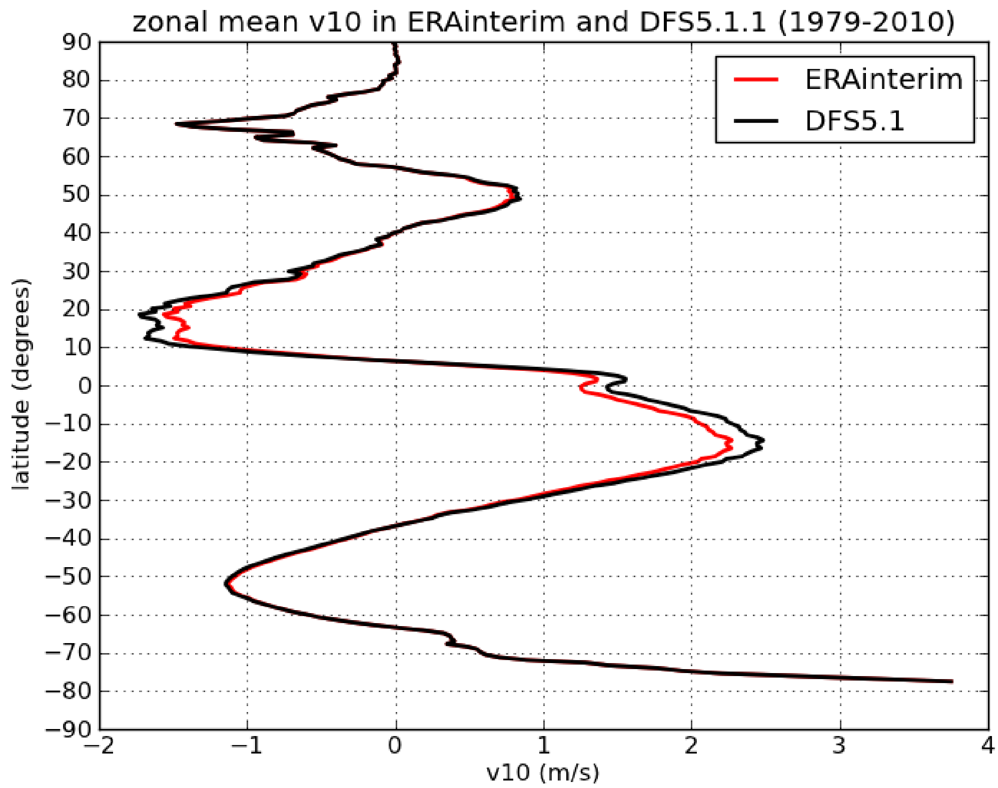

Figure 34: Zonal mean (1979-2010) v10 in DFS5.1 and original ERAinterim

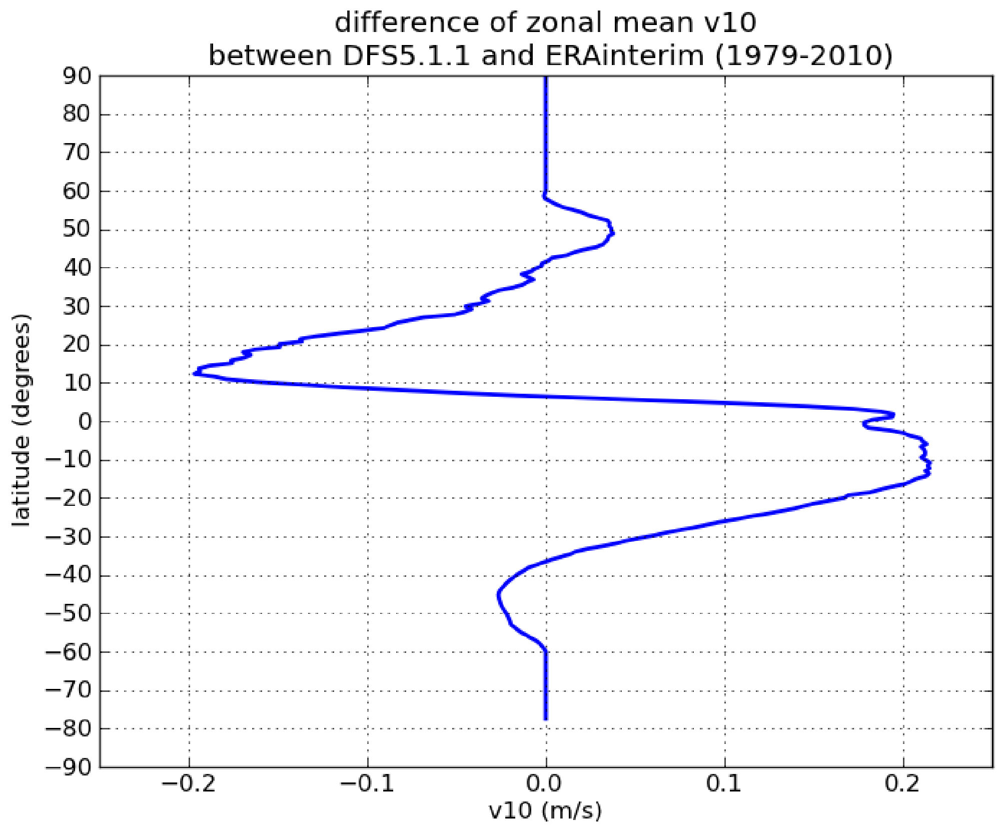

Figure 35: Difference between zonal mean (1979-2010) v10 between DFS5.1 and original ERAinterim

3.5 Downwelling shortwave radiation

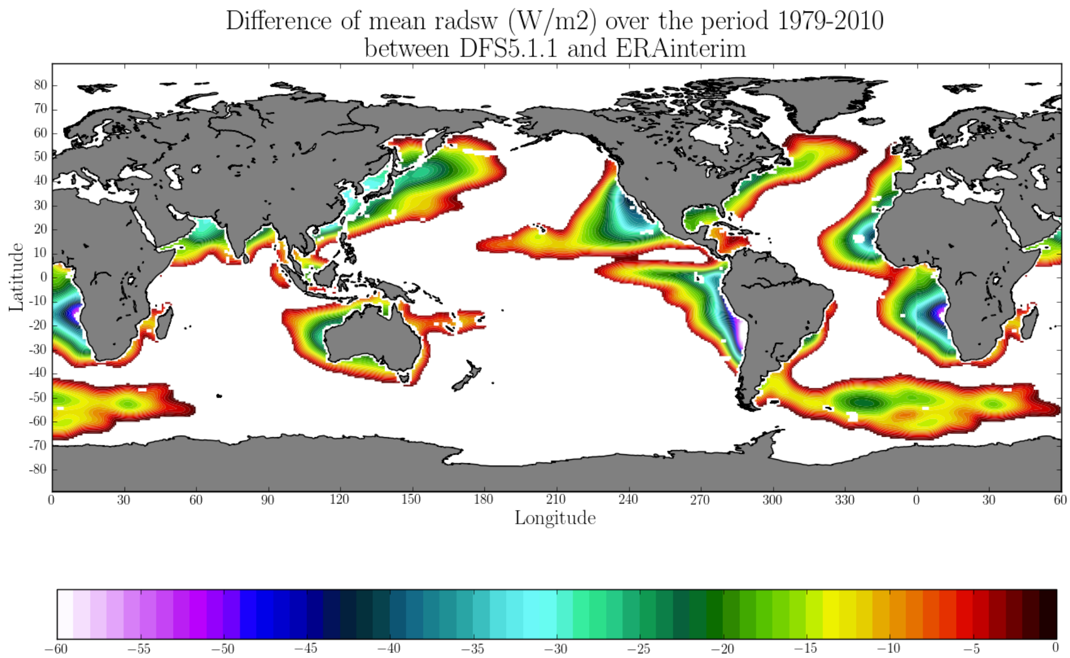

Figure 36: Difference between mean (1979-2010) radsw between DFS5.1 and original ERAinterim

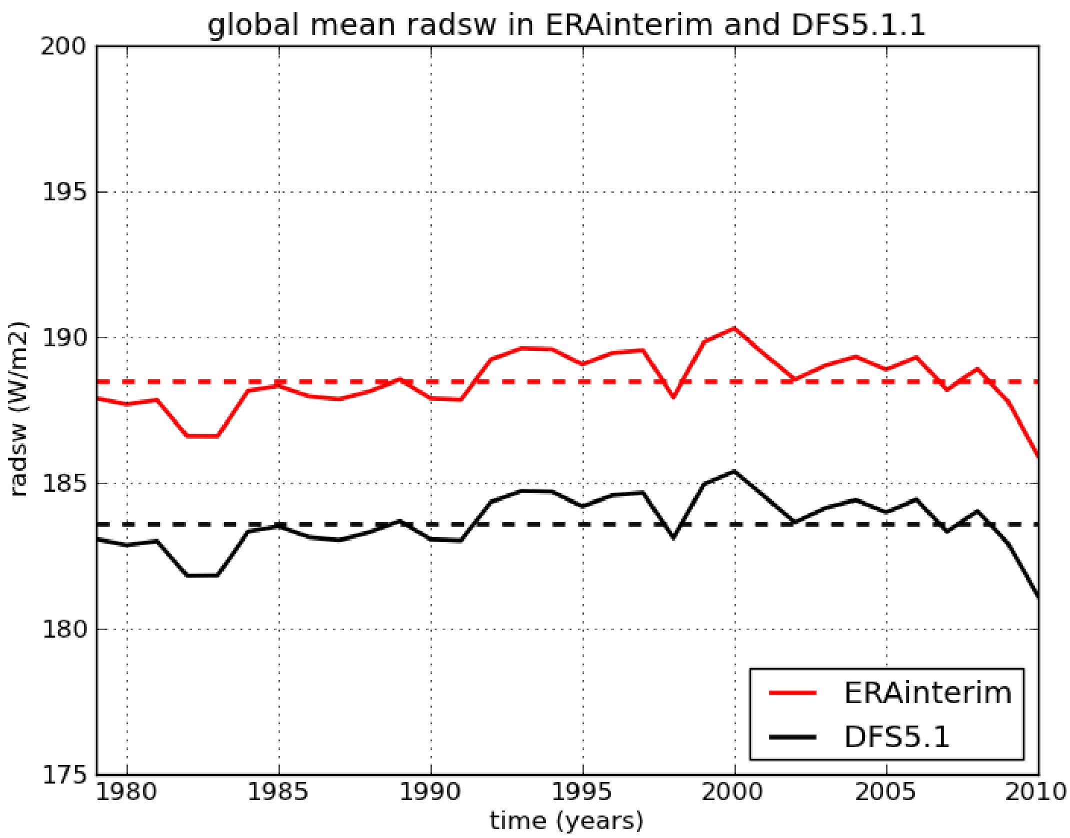

Figure 37: timeserie of annual mean radsw (global) in ERAinterim and DFS5.1

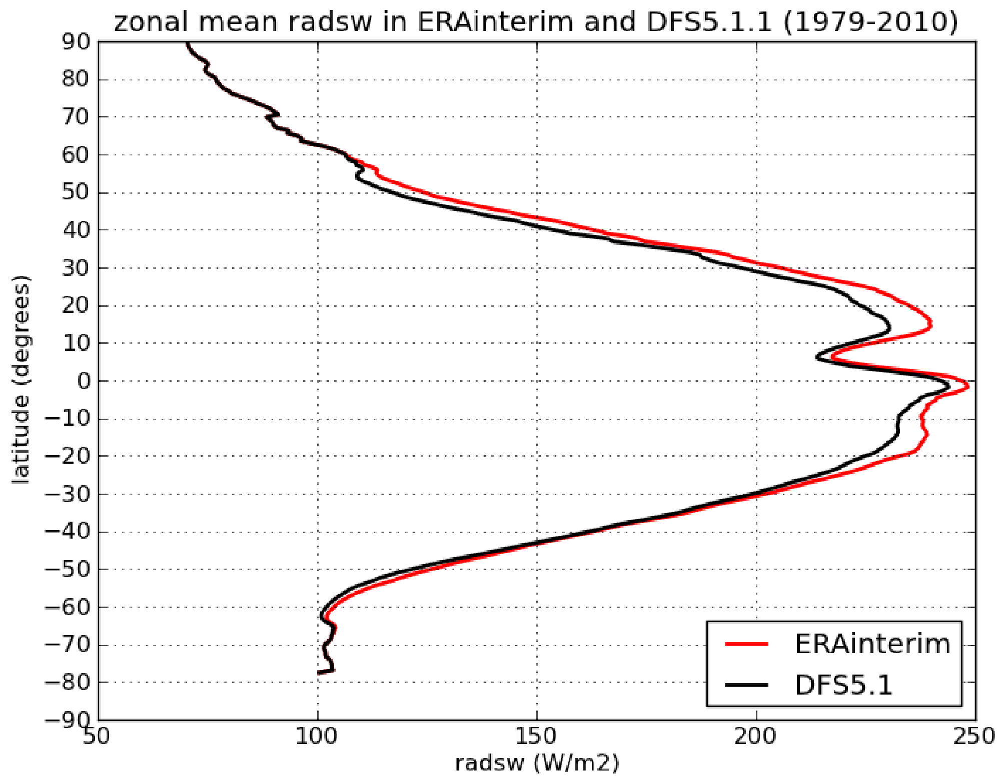

Figure 38: Zonal mean (1979-2010) radsw in DFS5.1 and original ERAinterim

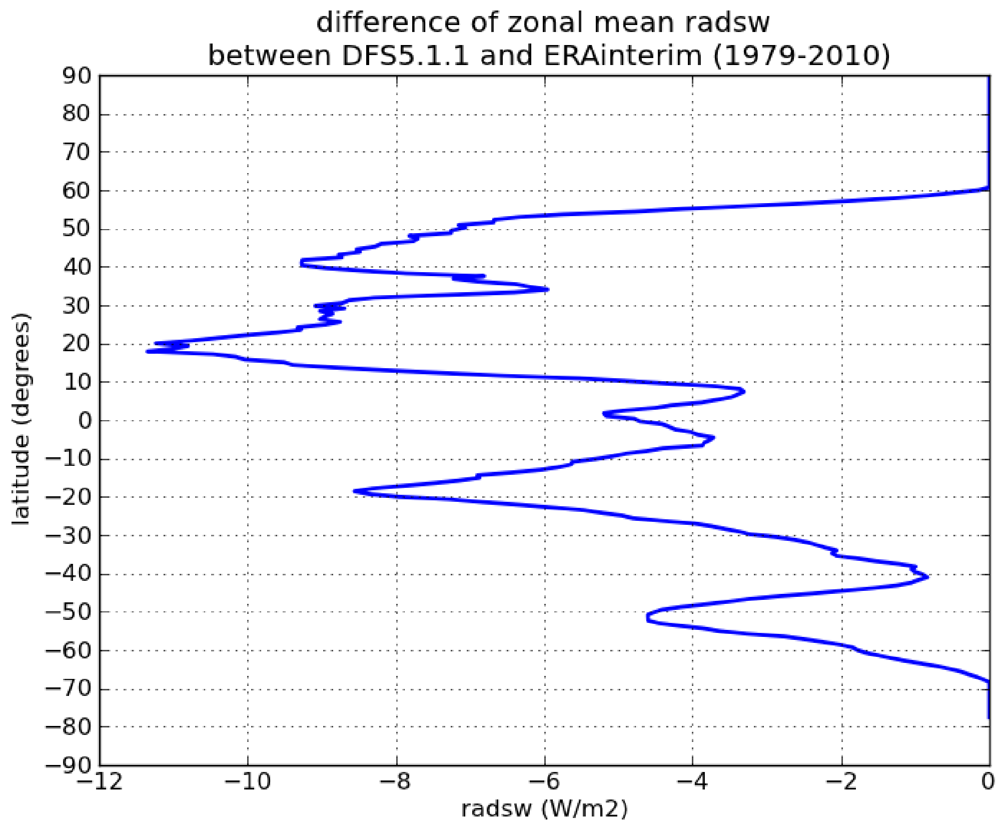

Figure 39: Difference between zonal mean (1979-2010) radsw between DFS5.1 and original ERAinterim

3.6 Downwelling longwave radiation

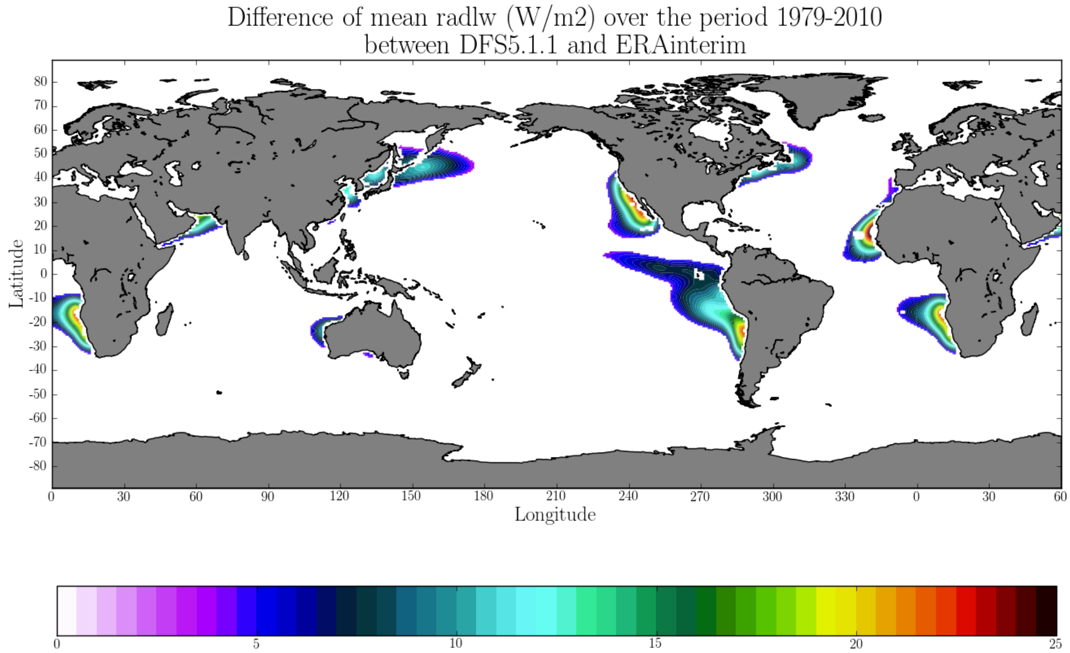

Figure 40: Difference between mean (1979-2010) radlw between DFS5.1 and original ERAinterim

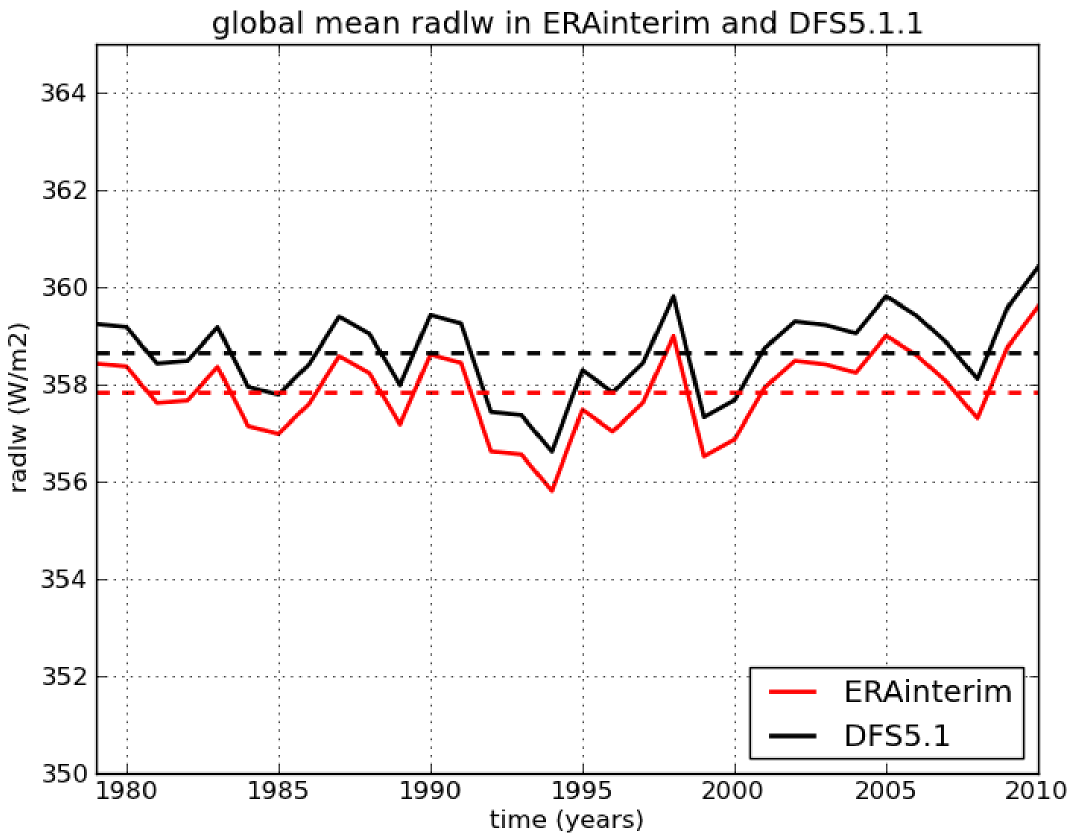

Figure 41: timeserie of annual mean radlw (global) in ERAinterim and DFS5.1

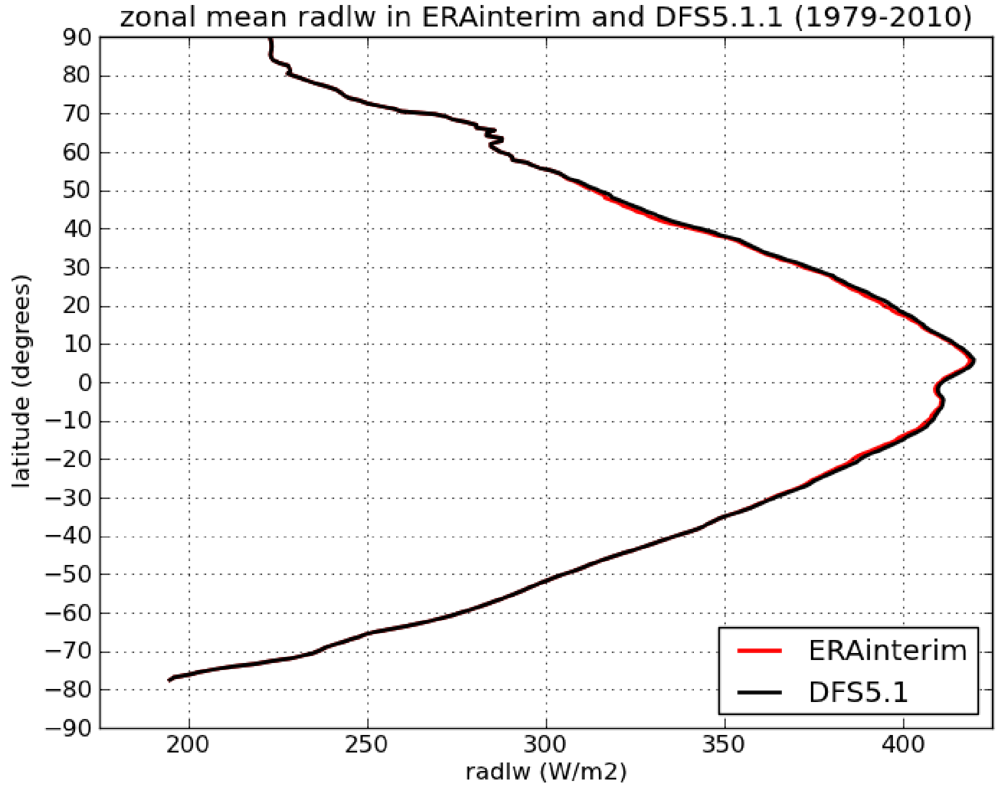

Figure 42: Zonal mean (1979-2010) radlw in DFS5.1 and original ERAinterim

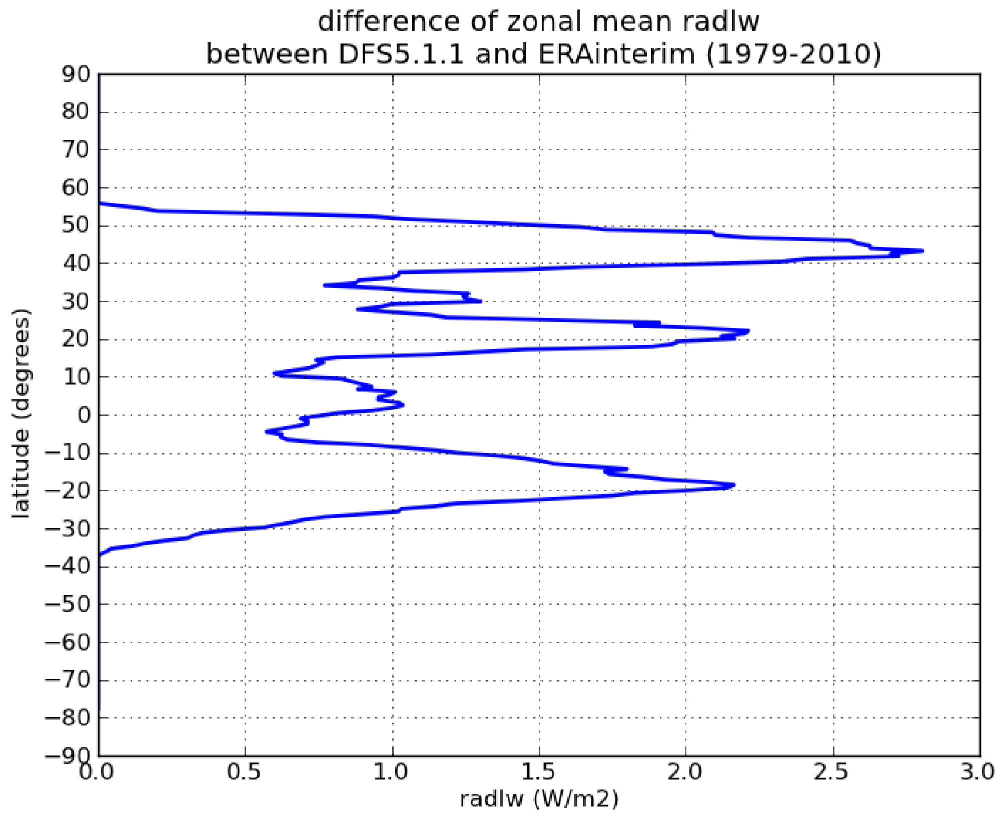

Figure 43: Difference between zonal mean (1979-2010) radlw between DFS5.1 and original ERAinterim

3.7 Total precipitation

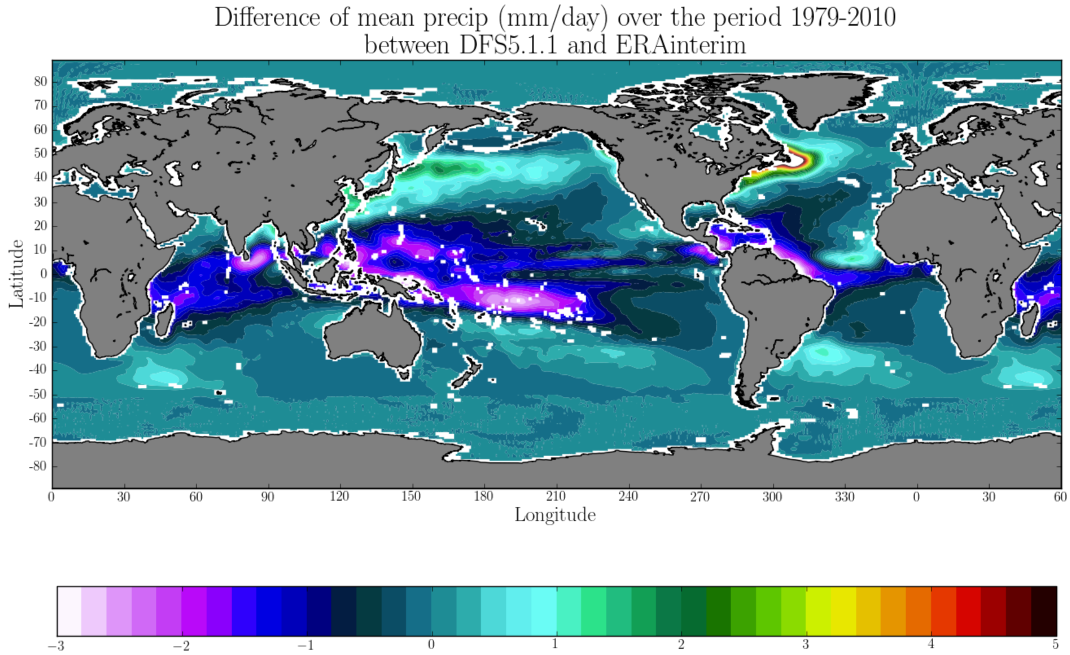

Figure 44: Difference between mean (1979-2010) precip between DFS5.1 and original ERAinterim

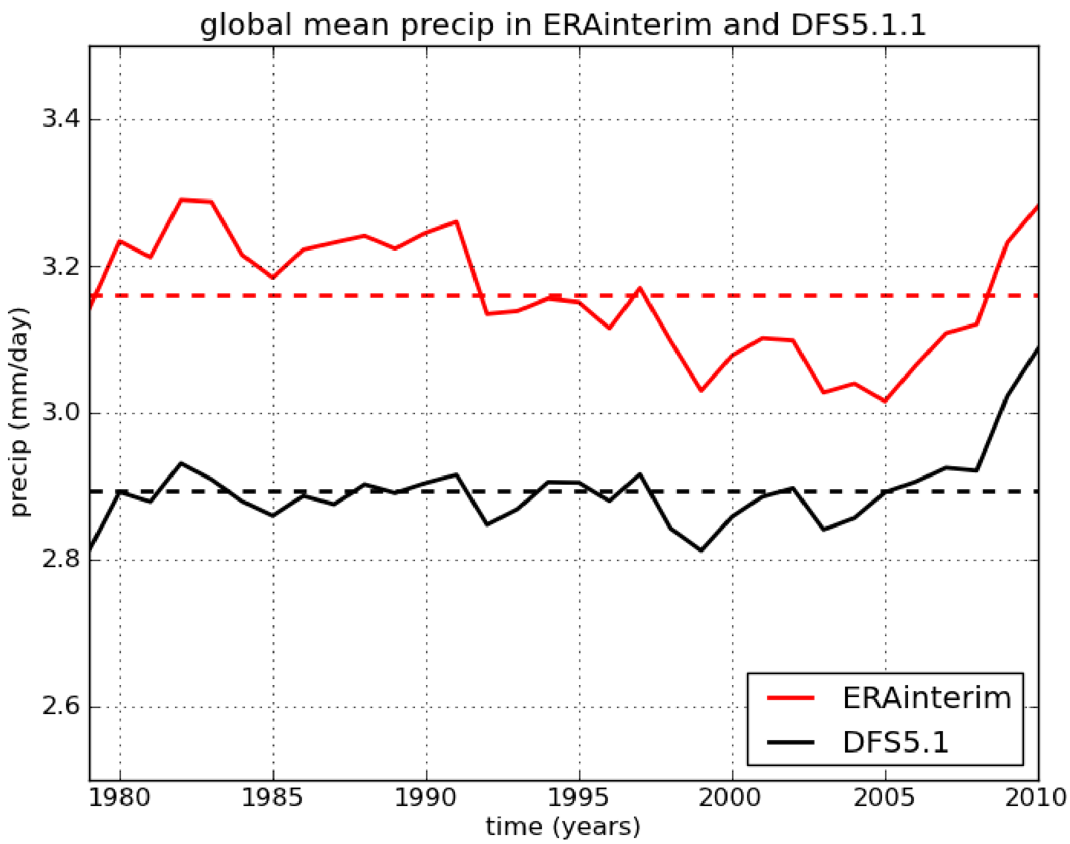

Figure 45: timeserie of annual mean precip (global) in ERAinterim and DFS5.1

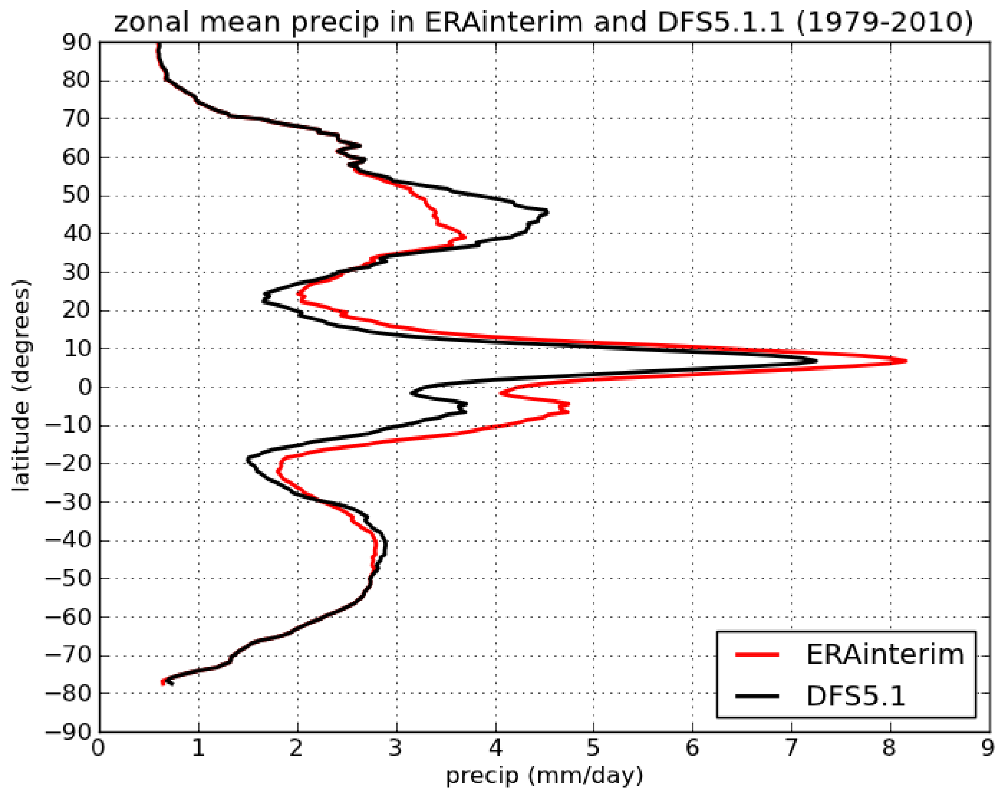

Figure 46: Zonal mean (1979-2010) precip in DFS5.1 and original ERAinterim

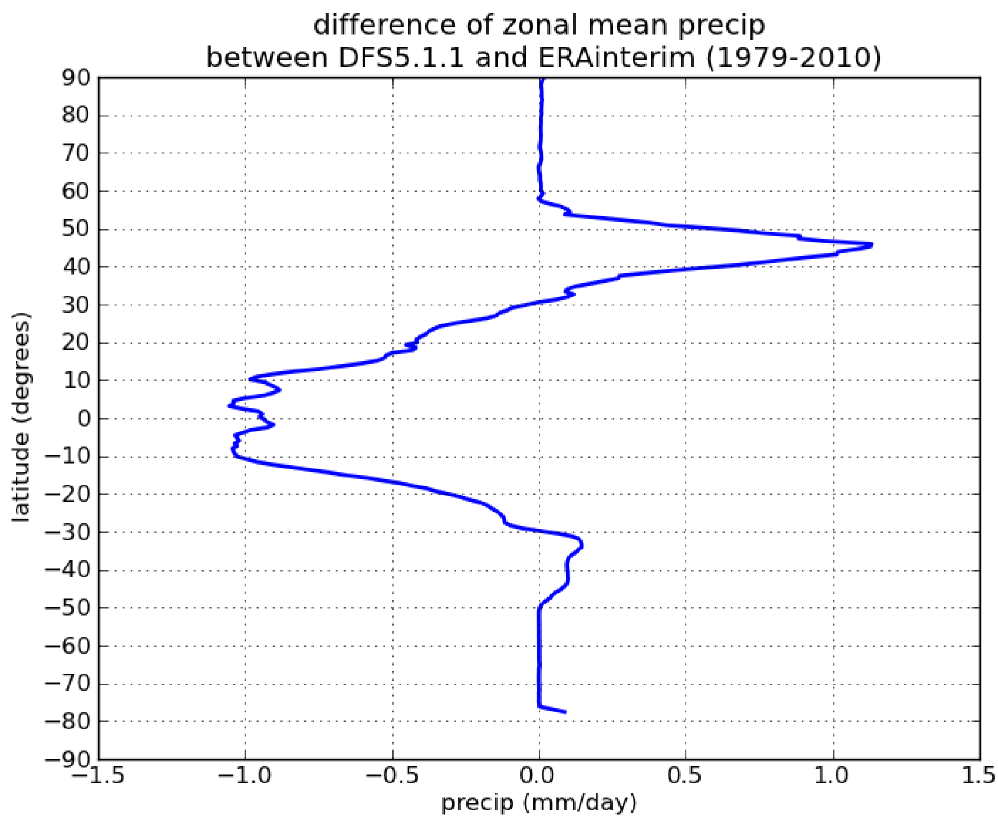

Figure 47: Difference between zonal mean (1979-2010) precip between DFS5.1 and original ERAinterim

4 Epilogue : conclusions and remarks

This section close the report and one year of work on the forcing fields. We will briefly summarize the modifications and discuss their implications on heat and freshwater fluxes. We will end with some remarks regarding freshwater balance. Figure 48 summarizes the differences between the spatially and time-averaged atmospheric variables. Air temperature has been lowered of 1.4° in the arctic and specific humidity has been corrected to conserve relative humidity. The wind have been strengthen especially in the zonal direction. The shortwave radiation has been decreased of 5 W/m2 partly compensated by an increase of 0.8 W/m2 of longwave radiation. Finally, precipitations have been detrended and decreased of 0.27 mm/day.

	ERAinterim	DFS5.1
t2 arctic (C)	-10.7	-12.1
q2 arctic (mg/kg)	2029	1896
u10 (m/s)	-0.31	-0.43
v10 (m/s)	0.21	0.24
radsw (W/m2)	188.5	183.6
radlw (W/m2)	357.84	358.65
precip (mm/day)	3.16	2.89

Figure 48: Means of atmospheric variables (global except t2 and q2, 1979-2010)

As the result, the net heat flux is now closer to balance (-2.24 W/m2 in DFS5.1 and 5.34 in ERA-interim) and the freshwater budget is less balanced due to enhanced evaporation and less precipitation. (see Figure 49). ERA-interim forced ORCA2 simulation without sea-surface salinity restoring has a freshening trend even if E-P-R is positive, which show the limits of the offline approach. The resulting forcing set has an important positive salt trend without restoring but a moderate one when restoring is applied.

	ERAinterim	DFS5.1
E-P (mm/day)	0.55	0.94
E-P-R (mm/day)	0.33	0.72
Qnet (W/m2)	5.34	-2.24

Figure 49: Mean freshwater and heat budget (global,1979-2010)

The freshwater balance can be further corrected using the multiplicative ratio on precipitations available in NEMO. A few sensitivity test have been performed to assess this issue. To bring the E-P to the original value of ERAinterim would require a correction by the multiplicative ratio of 1.13, this has been tested in an ORCA2 simulation and it leads to a major freshening of the model. Figure 50 shows a serie of experiments with DFS5.1 with several value of precipitation factor ranging from 1. to 1.09. Without online correction on precipitation the drift in salinity is positive, quite important (equivalent to a drop of 30cm in SSH) but stabilizes quickly. Other simulations show an initial positive drift then a negative trend occur for each simulation. Diagnostics on water fluxes (see figure 51) show that the more the E-P-R is unbalanced, the more the water damping brings the water flux close to a correct balance. When the E-P-R is closer to zero, the damping overshoots and leads to a freshening in the model. There are model-dependent differences in salinity drift : for example ORCA025.L75 forced by DFS4.3 shows a negative 3D-mean salinity trend whereas the 3D-mean salinity in ORCA2 in stable. Hence the adjustment of precipitations is an issue that cannot be solved easily.

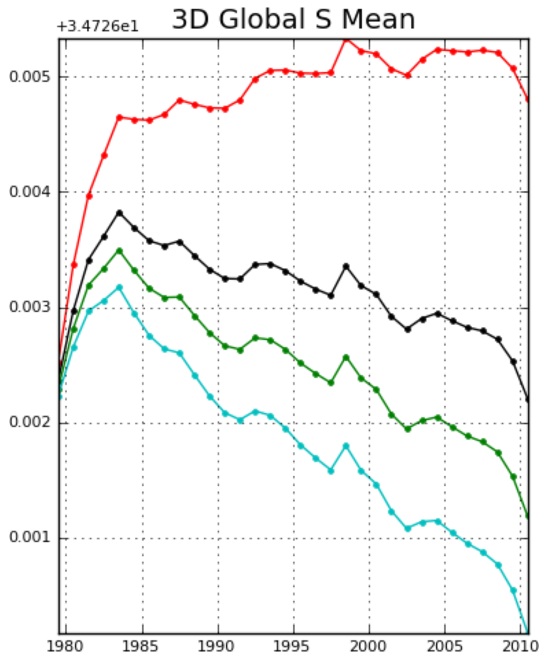

Figure 50: Salinity drift in ORCA246 model forced by DFS5.1 with precipitation multiplicative factor of 1.0 (red curve), 1.05 (black curve), 1.07 (green curve), 1.09 (cyan curve)

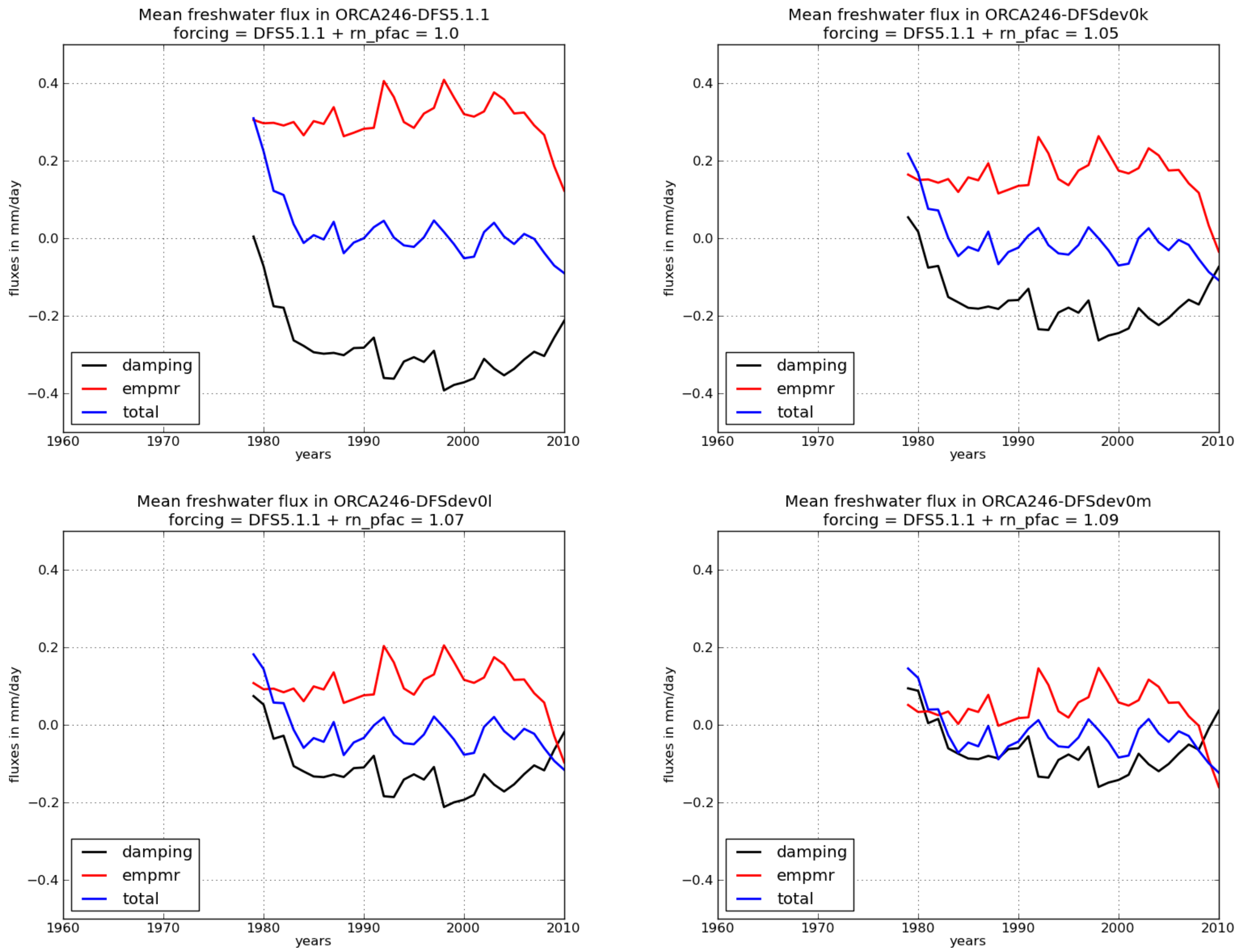

Figure 51: Evolution of E-P-R, damping and net water flux in DFS5.1 forced simulation with precipitation factor of 1.0 (top left), 1.05 (top right), 1.07 (bottom left) and 1.09 (bottom right)

Annex 1 : DFS5.1.2

Firstly, it is important to highlight that **DFS5.1.2 is the same that DFS5.1.1 except for the precipitations**. In this annex, we will thus describe the methodology for the computation of the new precipitations. The main issue with precipitations in DFS5.1.1 was the reinforcement of the precipitations in the north-western Atlantic. There is no evidence that this correction is needed and it produces a strong freshening of the water masses. The methodology thus proposed is :

- Apply Storto correction only at low latitudes (i.e. between 30°S and 30°N)
- Detrend the results (still in 3 periods, 1979-1991,1992-2004,2005-2010)
- Apply a global multiplicative factor (here 1.07 for freshwater balance)

Figure 52 and 53 show the resulting timeserie and zonal mean for these new precipitations compared to the original dataset (ERAinterim, red curve), DFS5.1.1 (black curve) and independent observations (GPCP 2.1, blue curve). We can see that the main issue at 45°N has been solved, the globally averaged precipitation range is bounded by GPCP and ERAinterim and there are no major trends except in the end of the period. The table hereafter summarize the different component involved in freshwater balance.

	ERAinterim	DFS5.1.1	DFS5.1.2
precipitation (mm/day)	3.16	2.89	3.00
evaporation (mm/day)	3.71	3.83	3.83
E-P (mm/day)	0.55	0.94	0.83
E-P-R (mm/day)	0.33	0.72	0.61

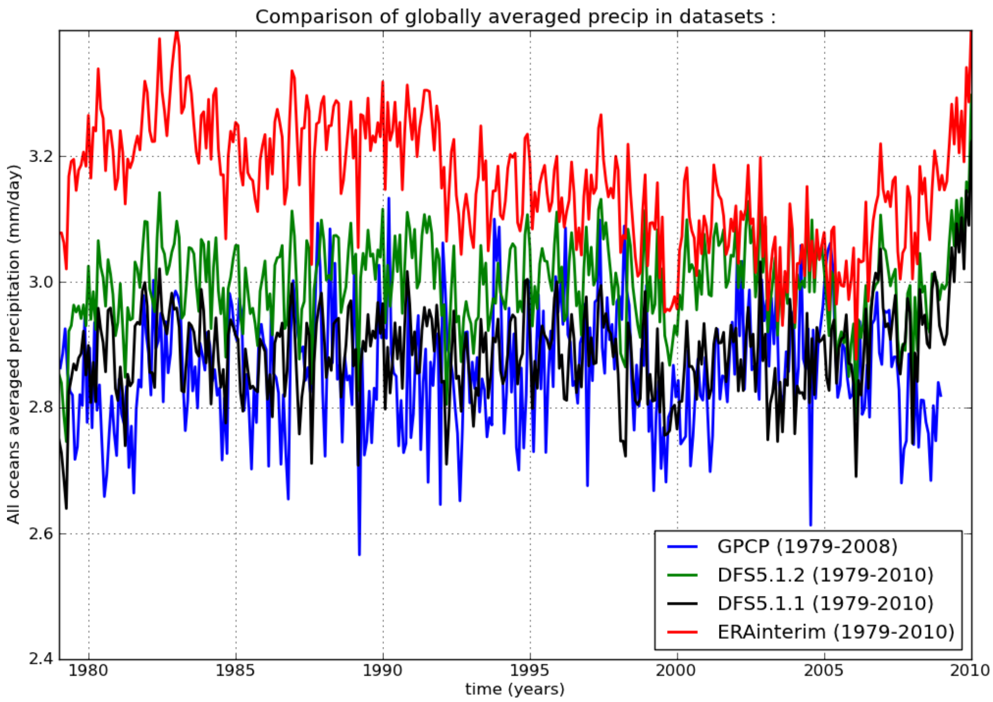

Figure 52: Mean precipitation (average on whole oceans) timeserie for ERAinterim (red), DFS5.1.1 (black), DFS5.1.2 (green) and GPCP 2.1 (blue)

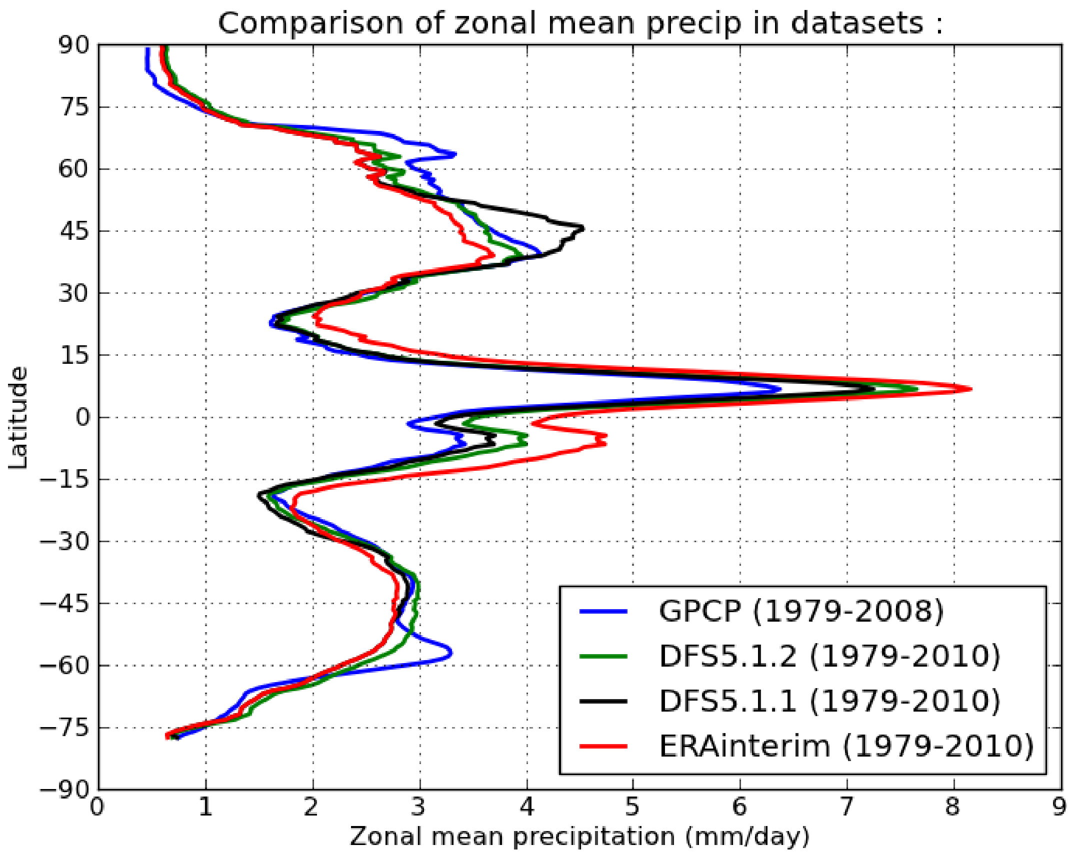

Figure 53: Mean precipitation (average on whole oceans and whole available period) zonal mean for ERAinterim (red), DFS5.1.1 (black), DFS5.1.2 (green) and GPCP 2.1 (blue)

Annex 2 : DFS5.1 extended

In this annex, we describe the strategy for producing an extended version of DFS5.1 spanning the period 1958-2010. ERAinterim and thus DFS5.1 are limited to the period 1979-2010. For 50 years long hindcasts, we have produced an extension for years 1958-1978 based on ERA40. We will first describe the strategy for radiative and freshwater fluxes. Then we will explain the computation for turbulent atmospheric variables.

Firstly, concerning radiative (shortwave and longwave downwelling radiation) and freshwater (total precipitation and snow) fluxes, the lack of observations before 1979 does not allow to produce an interannual set of fluxes. Thus, it was decided to use the climatology of DFS 5.1 over the period 1979-2010. This was also the strategy for DFS4.

We illustrate this extension with fluxes from DFS5.1.1 (only precipitation are different in DFS5.1.2). Figures 54, 55 and 56 show timeseries for shortwave, longwave and precipitation. As expected, the mean are values are identical and there is a lack of variability in longwave and precipitation.

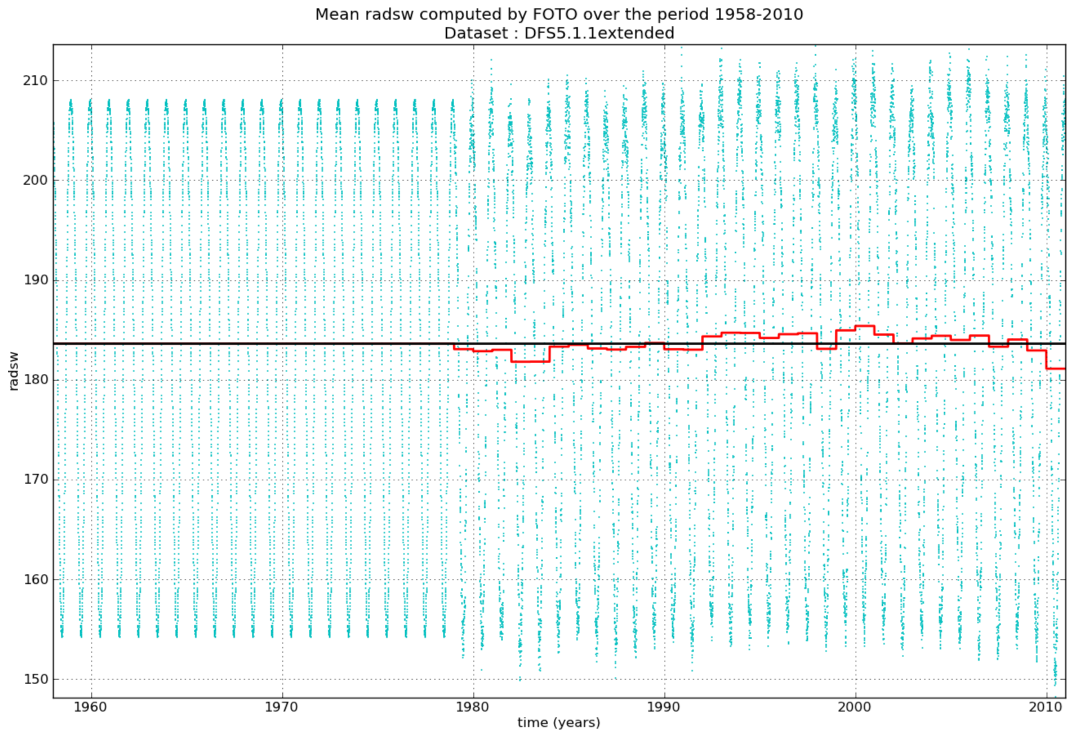

Figure 54: Timeserie for globally averaged shortwave radiation in extended DFS5.1.1

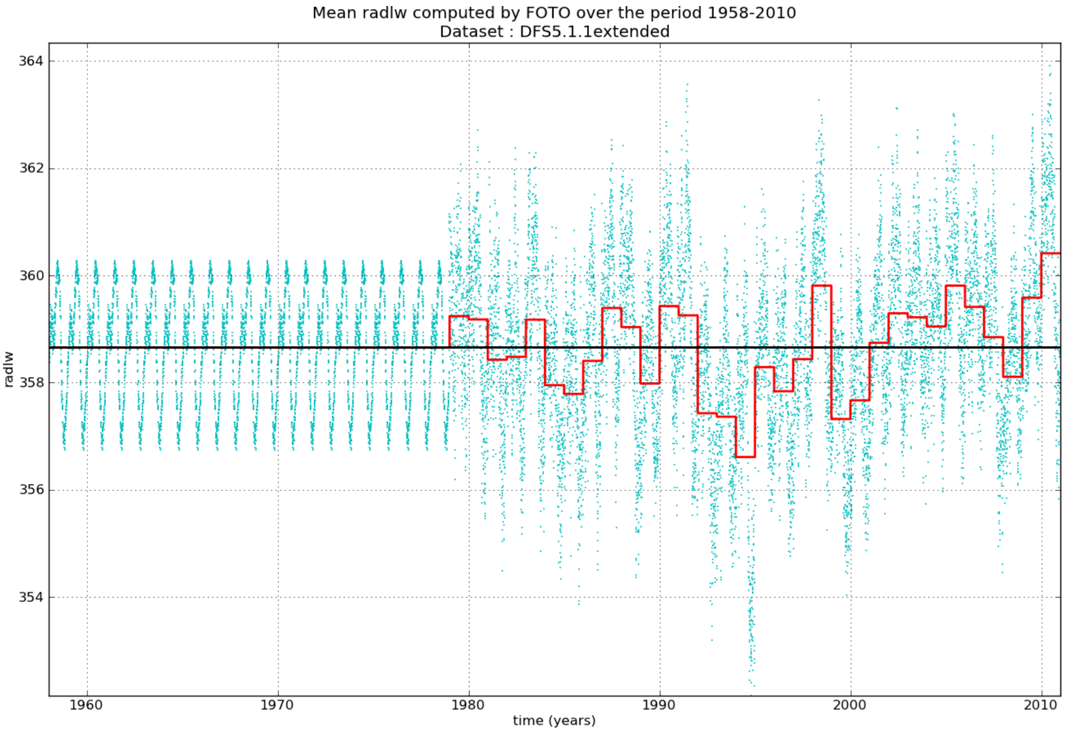

Figure 55: Timeserie for globally averaged longwave radiation in extended DFS5.1.1

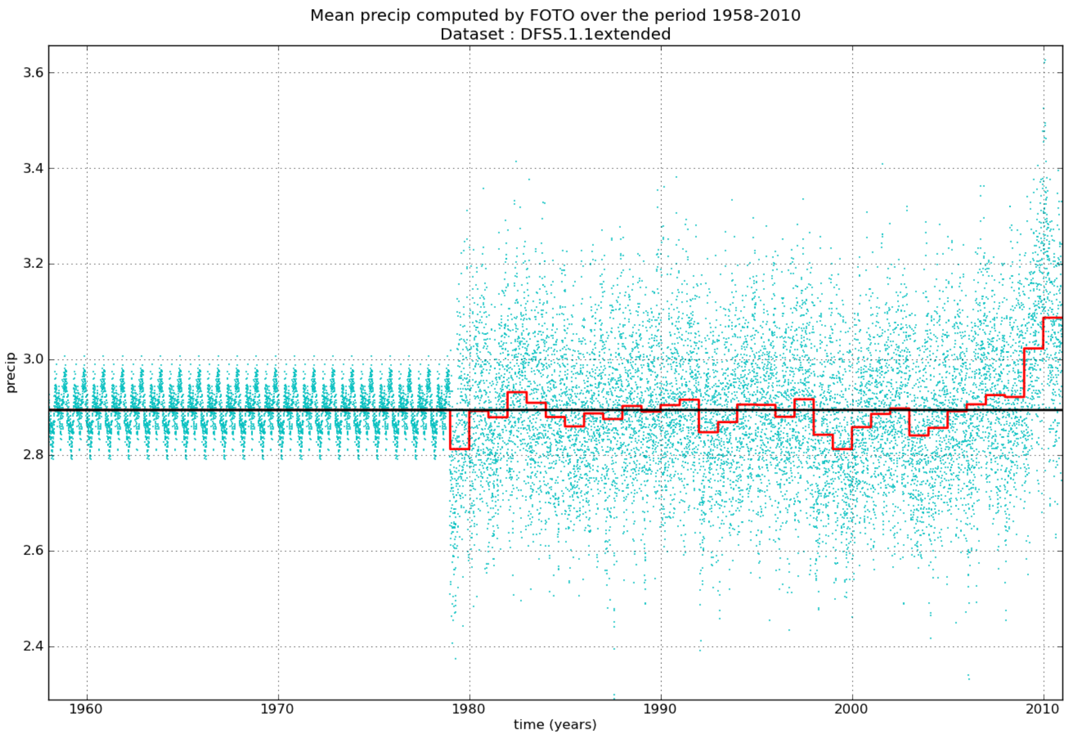

Figure 56: Timeserie for globally averaged total precipitation in extended DFS5.1.1

For turbulent atmospheric variables (t2, q2, u10 and v10), the strategy is much complex. We chose to use the information regarding synoptic scales contained into ERA40 and rescale it towards the means of our DFS5.1 dataset. This is done in several steps detailed below :

- 1. Compute the mean state for each variable : we produce a daily climatology for each DFS5.1 and ERA40 variable over the common period 1979-2001.
- 2. 6-hourly residues are computed for ERA40 over 1958-1978 : we remove from the ERA40 full fields the ERA40 daily climatology computed over 1979-2001.
- 3. ERA40 residues are interpolated to 3-hourly time frequency : to avoid changes in time frequency between the extended and standard periods, a linear interpolation is performed in time on the residues.
- 4. The full fields for DFS5.1 over 1958-1978 is recomposed from 3-hourly residues of ERA40 and the daily climatology of DFS5.1.

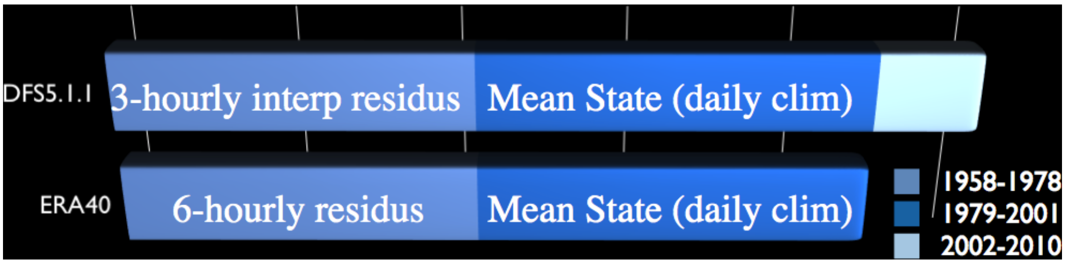

Figure 57: Strategy for atmospheric turbulent variables

The resulting timeseries for globally averaged atmospheric variables is shown in figures 58 to 61. There is a rather good continuity between the two periods 1958-1978 and 1979-2010 and no major drops in 1979. Though the effective time frequency over the period 1958-1978 is only 6 hours, the amplitude of the timeserie is rather similar for the two periods.

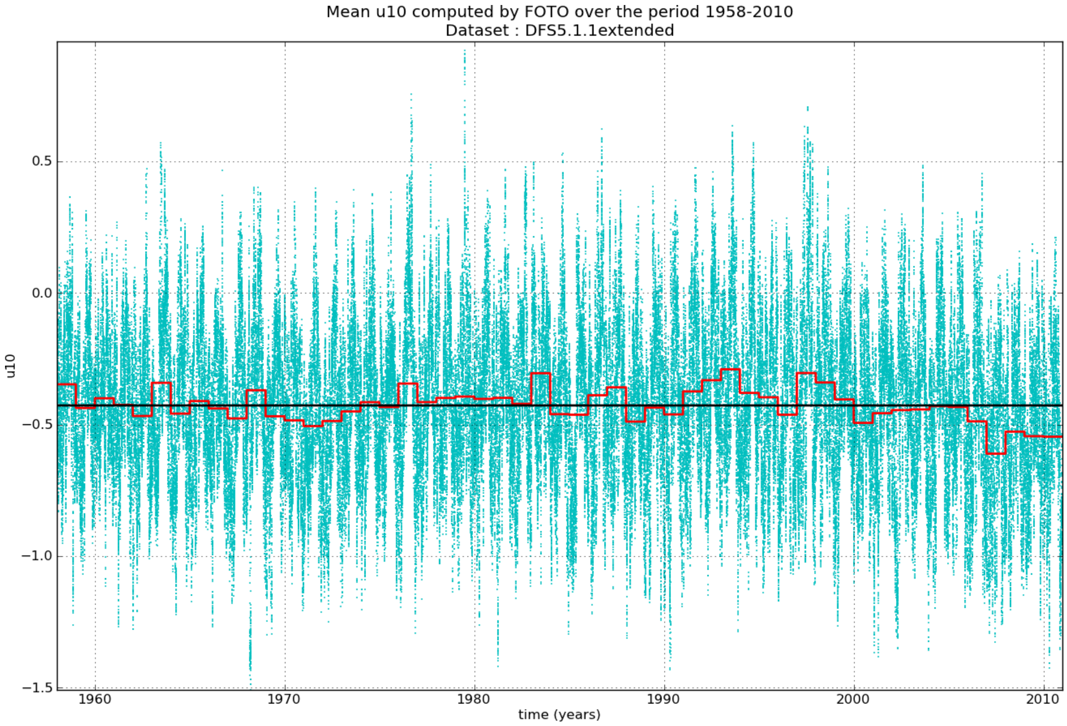

Figure 58: Timeserie for globally averaged total precipitation in extended DFS5.1

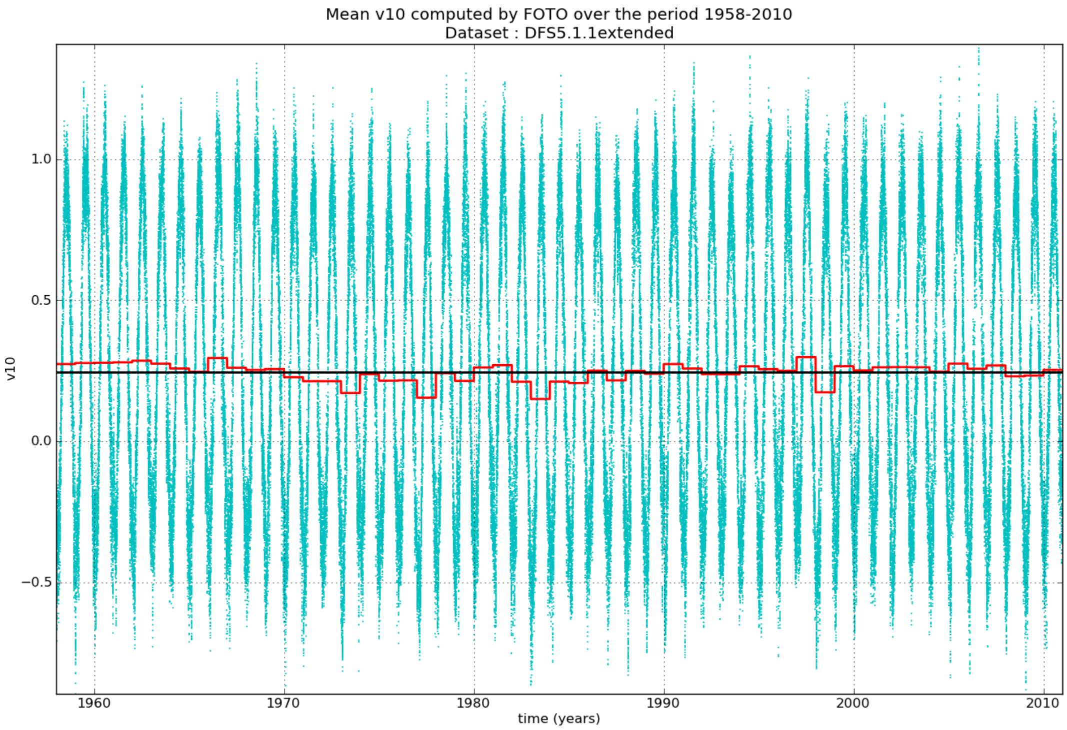

Figure 59: Timeserie for globally averaged total precipitation in extended DFS5.1

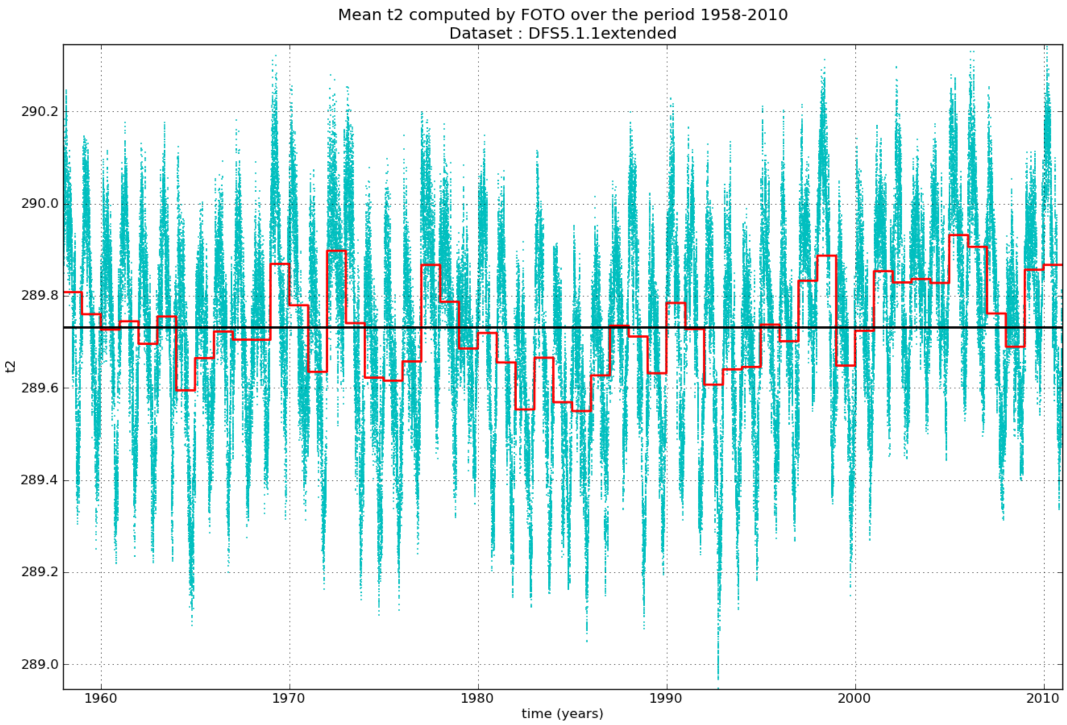

Figure 60: Timeserie for globally averaged total precipitation in extended DFS5.1

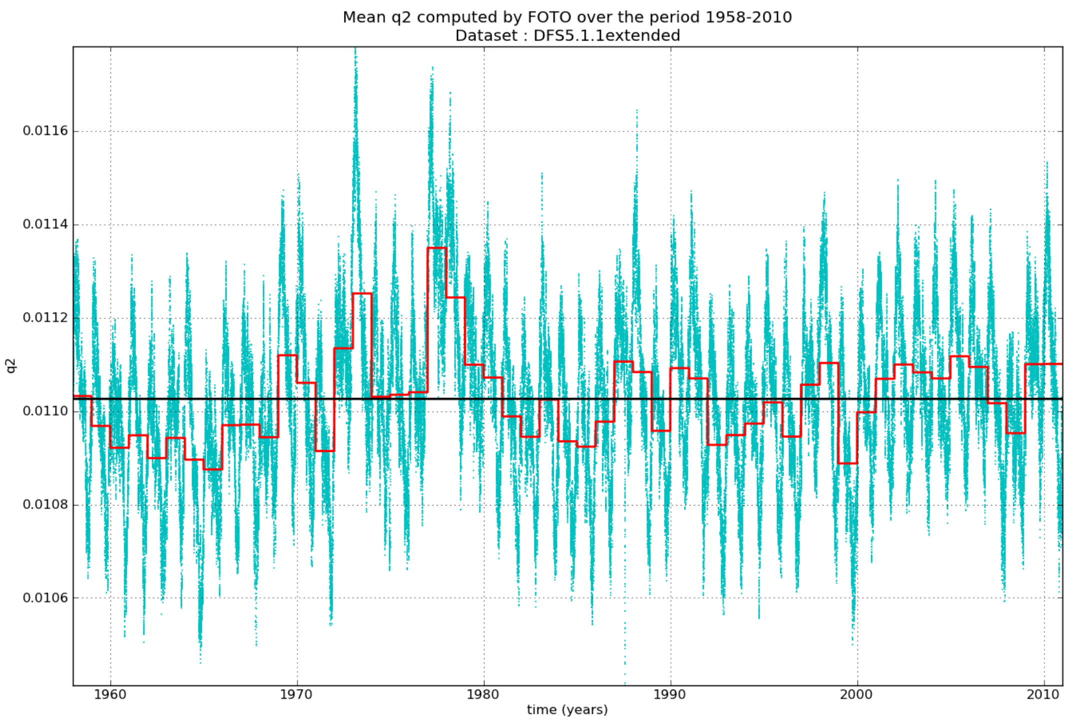

Figure 61: Timeserie for globally averaged total precipitation in extended DFS5.1

Bibliography

Brodeau et al., *An ERA40-based atmospheric forcing for global ocean circulation models*, **Ocean Modelling**, Volume 31, Issues 34, 2010, Pages 88-104, ISSN 1463-5003

Storto et al., *Interannual response of global ocean hindcasts to a satellite-based correction of precipitation fluxes*, **Ocean Science discussion paper**

Dee et al., *The ERA-Interim reanalysis: configuration and performance of the data assimilation system*, **Quart. J. R. Meteorol. Soc.**, Volume 137, Pages 553-597

Acknowledgments

The authors wish to thank Sergei Gulev, Laurent brodeau, Gilles Garric, Andrea Storto and Marion Meinvielle for their contribution : data or scientific discussions. The research leading to these results has received funding from the European Union's Seventh Framework Programme [FP7/2007-2013] under grant agreement n218812 (MyOcean). This work was part of workpackage 4.2.4.